The gene *cortex* controls mimicry and crypsis in butterflies and moths

Nicola J. Nadeau[1,2], Carolina Pardo-Diaz[3], Annabel Whibley[4,5], Megan A. Supple[2,6], Suzanne V. Saenko[4], Richard W. R. Wallbank[2,7], Grace C. Wu[8], Luana Maroja[9], Laura Ferguson[10], Joseph J. Hanly[2,7], Heather Hines[11], Camilo Salazar[3], Richard M. Merrill[2,7], Andrea J. Dowling[12], Richard H. ffrench-Constant[12], Violaine Llaurens[4], Mathieu Joron[4,13], W. Owen McMillan[2] & Chris D. Jiggins[7,2]

[1]Department of Animal and Plant Sciences, University of Sheffield, Western Bank, Sheffield, S10 2TN UK.

[2]Smithsonian Tropical Research Institute, Apartado Postal 0843-00153, Panamá, República de Panamá

[3]Biology Program, Faculty of Natural Sciences and Mathematics, Universidad del Rosario, Cra. 24 No 63C-69, Bogotá D.C., 111221, Colombia.

[4]Institut de Systématique, Evolution et Biodiversité (UMR 7205 CNRS, MNHN, UPMC, EPHE, Sorbonne Université), Museum National d'Histoire Naturelle, CP50, 57 rue Cuvier, 75005 Paris, France.

[5]Cell and Developmental Biology, John Innes Centre, Norwich, Norfolk NR4 7UH, UK.

[6]Research School of Biology, The Australian National University, 134 Linnaeus Way, Acton, ACT, 2601, Australia

[7]Department of Zoology, University of Cambridge, Downing Street, Cambridge, CB2 3EJ, UK

[8]Energy and Resources Group, University of California at Berkeley, California, 94720, USA.

[9]Department of Biology, Williams College, Williamstown, Massachusetts 01267, USA[10]Department of Zoology, University of Oxford, South Parks Rd, Oxford, OX1 3PS, UK

[11]Penn State University, 517 Mueller, University Park, Pennsylvania 16802, USA.

[12]School of Biosciences, University of Exeter in Cornwall, Penryn, Cornwall TR10 9FE, UK.

[13]Centre d'Ecologie Fonctionnelle et Evolutive (CEFE, UMR 5175 CNRS, Université de Montpellier, Université Paul-Valéry Montpellier, EPHE), 1919 route de Mende, 34293 Montpellier, France

The wing patterns of butterflies and moths (Lepidoptera) are diverse and striking examples of evolutionary diversification by natural selection[1,2]. Lepidopteran wing colour patterns are a key innovation, consisting of arrays of coloured scales. We still lack a general understanding of how these patterns are controlled and if there is any commonality across the 160,000 moth and 17,000 butterfly species. Here, we identify a gene, *cortex*, through fine-scale mapping using population genomics and gene expression analyses, which regulates pattern switches in multiple species across the mimetic radiation in *Heliconius* butterflies. *cortex* belongs to a fast evolving subfamily of the otherwise highly conserved fizzy family of cell cycle regulators[3], suggesting that it most likely regulates pigmentation patterning through regulation of scale cell development. In parallel with findings in the peppered moth (*Biston betularia*)[4], our results suggest that this mechanism is common within Lepidoptera and that *cortex* has become a major target for natural selection acting on colour and pattern variation in this group of insects.

In *Heliconius*, there is a major effect locus, *Yb*, that controls a diversity of colour pattern elements across the genus. It is the only locus in *Heliconius* that regulates all scale types and colours, including the diversity of white and yellow pattern elements in the two co-mimics *H. melpomene* (*Hm*) and *H. erato* (*He*), but also whole wing variation in black, yellow, white, and orange/red elements in *H. numata* (*Hn*)[5–7]. In addition, genetic variation underlying the *Bigeye* wing pattern mutation in *Bicyclus anynana*, melanism in the peppered moth, *Biston betularia*, and melanism and patterning differences in the silkmoth, *Bombyx mori*, have all been localised to homologous genomic regions[8–10] (Fig 1). Therefore, this genomic region appears to contain one or more genes that act as major regulators of wing pigmentation and patterning across the Lepidoptera.

Previous mapping of this locus in *He, Hm* and *Hn* identified a genomic interval of ~1Mb[11–13] (Extended Data Table 1), which also overlaps with the 1.4Mb region containing the *carbonaria* locus in *B. betularia*[9] and a 100bp non-coding region containing the *Ws* mutation in *B. mori*[10] (Fig 1). We took a population genomics approach to identify single nucleotide polymorphisms (SNPs) most strongly associated with phenotypic variation within the ~1Mb *Heliconius* interval. The diversity of wing patterning in *Heliconius* arises from divergence at wing pattern loci[7], while convergent patterns generally involve the same loci and sometimes even the same alleles[14–16]. We used this pattern of divergence and sharing to identify SNPs associated with colour pattern elements across many individuals from a wide diversity of colour pattern phenotypes (Fig 2).

In three separate *Heliconius* species, our analysis consistently implicated the gene *cortex* as being involved in adaptive differences in wing colour pattern. In *He* the strongest associations with the presence of a yellow hindwing bar were centred around the genomic region containing *cortex* (Fig 2A). We identified 108 SNPs that were fixed for one allele in *He favorinus*, and fixed for the alternative allele in all individuals lacking the yellow bar, the majority of which were in introns of *cortex* (Extended Data Table 2). 15 SNPs showed a similar fixed pattern for *He demophoon*, which also has a yellow bar. These were non-overlapping with those in *He favorinus*, consistent with the hypothesis that this phenotype evolved independently in the two disjunct populations[17].

Previous work has suggested that alleles at the *Yb* locus are shared between *Hm* and the closely related species *H. timareta*, and also the more distantly related species *H. elevatus*, resulting in mimicry between these species[18]. Across these species, the strongest associations with the yellow hindwing bar phenotype were again found at *cortex* (Fig 2D, Extended Data Fig 1A and Table 3). Similarly, the strongest associations with the yellow forewing band were found around the 5' UTRs of *cortex* and gene *HM00036*, an orthologue of *D.*

melanogaster washout gene. A single SNP ~17kb upstream of *cortex* (the closest gene) was perfectly associated with the yellow forewing band across all *Hm*, *H. timareta* and *H. elevatus* individuals (Extended Data Fig 1A, Fig 2 and Table 3). We found no fixed coding sequence variants at *cortex* in a larger sample (43-61 individuals) of *Hm aglaope* and *Hm amaryllis* (Extended Data Figure 3, Supplementary Information), which differ in *Yb* controlled phenotypes[19], suggesting that functional variants are likely to be regulatory rather than coding. We found extensive transposable element variation around *cortex* but it is unclear if any of these associate with phenotype (Extended Data Figure 3 and Table 4; Supplementary Information).

Finally, in *Hn* large inversions at the *P* supergene locus (Fig 1) are associated with different morphs[13]. There is a steep increase in genotype-by-phenotype association at the breakpoint of inversion 1, consistent with the role of these inversions in reducing recombination (Fig 2E). However, the *bicoloratus* morph can recombine with all other morphs across one or the other inversion, permitting finer-scale association mapping of this region. As in *He* and *Hm*, this analysis showed a narrow region of associated SNPs corresponding exactly to the *cortex* gene (Fig 2E), again with the majority of SNPs in introns (Extended Data Table 2). This associated region does not correspond to any other known genomic feature, such as an inversion or inversion breakpoint.

To determine whether sequence variants around *cortex* were regulating its expression we investigated gene expression across the *Yb* locus. We used a custom designed microarray including probes from all predicted genes in the *H. melpomene* genome[18], as well as probes tiled across the central portion of the *Yb* locus, focussing on two naturally hybridising *Hm* races (*plesseni* and *malleti*) that differ in *Yb* controlled phenotypes[7]. *cortex* was the only gene across the entire interval to show significant expression differences both between races with different wing patterns and between wing sections with different pattern elements (Fig 3).

This finding was reinforced in the tiled probe set, where we observed strong differences in expression of *cortex* exons and introns but few differences outside this region (Extended Data Table 2). *cortex* expression was higher in *Hm malleti* than *Hm plesseni* in all three wing sections used (but not eyes) (Fig 3C; Extended Data Fig 4C). When different wing sections were compared within each race, *cortex* expression in *Hm malleti* was higher in the distal section that contains the *Yb* controlled yellow forewing band, consistent with *cortex* producing this band. In contrast, *Hm plesseni*, which lacks the yellow band, had higher *cortex* expression in the proximal forewing section (Fig 3F; Extended Data Fig 4J). Expression differences were found only in day 1 and day 3 pupal wings rather than day 5 or day 7 (Extended Data Fig 4), similar to the pattern observed previously for the transcription factor *optix*[20].

Differential expression was not confined to the exons of *cortex*; the majority of differentially expressed probes in the tiling array corresponded to *cortex* introns (Fig 3). This does not appear to be due to transposable element variation (Extended Data Table 2), but may be due to elevated background transcription and unidentified splice variants. RT-PCR revealed a diversity of splice variants (Extended Data Fig 5), and sequenced products revealed 8 non-constitutive exons and 6 variable donor/acceptor sites, but this was not exhaustive (Supplementary Information). We cannot rule out the possibility that some of the differentially expressed intronic regions could be distinct non-coding RNAs. However, qRT-PCR in other hybridising races with divergent *Yb* alleles (*aglaope/amaryllis* and *rosina/melpomene)* also identified expression differences at *cortex* and allele-specific splicing differences between both pairs of races (Extended Data Figs 1 and 5, Supplementary Information).

Finally, *in situ* hybridisation of *cortex* in final instar larval hindwing discs showed expression in wing regions fated to become black in the adult wing, most strikingly in their

129 correspondence to the black patterns on adult *Hn* wings (Fig 4). In contrast, the array results
130 from pupal wings were suggestive of higher expression in non-melanic regions. This may
131 suggest that *cortex* is upregulated at different time-points in wing regions fated to become
132 different colours.

133 Overall, *cortex* shows significant differential expression and is the only gene in the candidate
134 region to be consistently differentially expressed in multiple race comparisons and between
135 differently patterned wing regions. Coupled with the strong genotype-by-phenotype
136 associations across multiple independent lineages (Extended Data Table 1), this strongly
137 implicates *cortex* as a major regulator of colour and pattern. However, we have not excluded
138 the possibility that other genes in this region also influence pigmentation patterning. A
139 prominent role for *cortex* is also supported by studies in other taxa; our identification of
140 distant 5' untranslated exons of *cortex* (Supplementary Information) suggests that the 100bp
141 interval containing the *Ws* mutation in *B. mori* is likely to be within an intron of *cortex* and
142 not in intergenic space as previously thought[10]. In addition, fine-mapping and gene
143 expression also implicate *cortex* as controlling melanism in the peppered moth[4].

144 It seems likely that *cortex* controls pigmentation patterning through control of scale cell
145 development. The *cortex* gene falls in an insect specific lineage within the fizzy/CDC20
146 family of cell cycle regulators (Extended Data Fig 6A). The phylogenetic tree of the gene
147 family highlighted three major orthologous groups, two of which have highly conserved
148 functions in cell cycle regulation mediated through interaction with the anaphase promoting
149 complex/cyclosome (APC/C)[3,21]. The third group, cortex, is evolving rapidly, with low amino
150 acid identity between *D. melanogaster* and *Hm* cortex (14.1%), contrasting with much higher
151 identities for orthologues between these species in the other two groups (fzy, 47.8% and
152 rap/fzr,47.2%, Extended Data Fig 6A). *Drosophila melanogaster* cortex acts through a

similar mechanism to fzy in order to control meiosis in the female germ line[22–24]. *Hm* cortex also has some conservation of the fizzy family C-box and IR elements (Supplementary Information) that mediate binding to the APC/C[23], suggesting that it may have retained a cell cycle function, although we found that expressing *Hm cortex* in *D. melanogaster* wings produced no detectable effect (Extended Data Fig 6, Supplementary Information).

Previously identified butterfly wing patterning genes have been transcription factors or signalling molecules[20,25]. Developmental rate has long been thought to play a role in lepidopteran patterning[26,27], but *cortex* was not a likely *a priori* candidate, because its *Drosophila* orthologue has a highly specific function in meiosis[23]. The recruitment of *cortex* to wing patterning appears to have occurred before the major diversification of the Lepidoptera and this gene has repeatedly been targeted by natural selection[1,7,9,28] to generate both cryptic[4] and aposematic patterns.

References

1. Cook, L. M., Grant, B. S., Saccheri, I. J. & Mallet, J. Selective bird predation on the peppered moth: the last experiment of Michael Majerus. *Biol. Lett.* **8,** 609–612 (2012).
2. Jiggins, C. D. Ecological Speciation in Mimetic Butterflies. *BioScience* **58,** 541–548 (2008).
3. Dawson, I. A., Roth, S. & Artavanis-Tsakonas, S. The Drosophila Cell Cycle Gene fizzy Is Required for Normal Degradation of Cyclins A and B during Mitosis and Has Homology to the CDC20 Gene of Saccharomyces cerevisiae. *J. Cell Biol.* **129,** 725–737 (1995).
4. Van't Hof, A. E. *et al.* The industrial melanism mutation in British peppered moths is a transposable element. *Nature* **This issue,**

5. Joron, M. *et al.* A Conserved Supergene Locus Controls Colour Pattern Diversity in Heliconius Butterflies. *PLoS Biol.* **4,** (2006).
6. Sheppard, P. M., Turner, J. R. G., Brown, K. S., Benson, W. W. & Singer, M. C. Genetics and the Evolution of Muellerian Mimicry in Heliconius Butterflies. *Philos. Trans. R. Soc. Lond. B. Biol. Sci.* **308,** 433–610 (1985).
7. Nadeau, N. J. *et al.* Population genomics of parallel hybrid zones in the mimetic butterflies, H. melpomene and H. erato. *Genome Res.* **24,** 1316–1333 (2014).
8. Beldade, P., Saenko, S. V., Pul, N. & Long, A. D. A Gene-Based Linkage Map for Bicyclus anynana Butterflies Allows for a Comprehensive Analysis of Synteny with the Lepidopteran Reference Genome. *PLoS Genet* **5,** e1000366 (2009).
9. van't Hof, A. E., Edmonds, N., Dalíková, M., Marec, F. & Saccheri, I. J. Industrial Melanism in British Peppered Moths Has a Singular and Recent Mutational Origin. *Science* **332,** 958 –960 (2011).
10. Ito, K. *et al.* Mapping and recombination analysis of two moth colour mutations, Black moth and Wild wing spot, in the silkworm Bombyx mori. *Heredity* (2015). doi:10.1038/hdy.2015.69
11. Counterman, B. A. *et al.* Genomic Hotspots for Adaptation: The Population Genetics of Müllerian Mimicry in Heliconius erato. *PLoS Genet.* **6,** e1000796 (2010).
12. Ferguson, L. *et al.* Characterization of a hotspot for mimicry: assembly of a butterfly wing transcriptome to genomic sequence at the HmYb/Sb locus. *Mol. Ecol.* **19,** 240–254 (2010).
13. Joron, M. *et al.* Chromosomal rearrangements maintain a polymorphic supergene controlling butterfly mimicry. *Nature* **477,** 203–206 (2011).
14. Hines, H. M. *et al.* Wing patterning gene redefines the mimetic history of Heliconius butterflies. *Proc. Natl. Acad. Sci.* **108,** 19666–19671 (2011).

15. Pardo-Diaz, C. *et al.* Adaptive Introgression across Species Boundaries in Heliconius Butterflies. *PLoS Genet* **8,** e1002752 (2012).
16. Wallbank, R. W. R. *et al.* Evolutionary Novelty in a Butterfly Wing Pattern through Enhancer Shuffling. *PLoS Biol* **14,** e1002353 (2016).
17. Maroja, L. S., Alschuler, R., McMillan, W. O. & Jiggins, C. D. Partial Complementarity of the Mimetic Yellow Bar Phenotype in Heliconius Butterflies. *PLoS ONE* **7,** e48627 (2012).
18. The Heliconius Genome Consortium. Butterfly genome reveals promiscuous exchange of mimicry adaptations among species. *Nature* **487,** 94–98 (2012).
19. Mallet, J. The Genetics of Warning Colour in Peruvian Hybrid Zones of Heliconius erato and H. melpomene. *Proc. R. Soc. Lond. B Biol. Sci.* **236,** 163–185 (1989).
20. Reed, R. D. *et al.* optix Drives the Repeated Convergent Evolution of Butterfly Wing Pattern Mimicry. *Science* **333,** 1137 –1141 (2011).
21. Barford, D. Structural insights into anaphase-promoting complex function and mechanism. *Philos. Trans. R. Soc. B Biol. Sci.* **366,** 3605–3624 (2011).
22. Chu, T., Henrion, G., Haegeli, V. & Strickland, S. Cortex, a Drosophila gene required to complete oocyte meiosis, is a member of the Cdc20/fizzy protein family. *genesis* **29,** 141–152 (2001).
23. Pesin, J. A. & Orr-Weaver, T. L. Developmental Role and Regulation of cortex, a Meiosis-Specific Anaphase-Promoting Complex/Cyclosome Activator. *PLoS Genet* **3,** e202 (2007).
24. Swan, A. & Schüpbach, T. The Cdc20/Cdh1-related protein, Cort, cooperates with Cdc20/Fzy in cyclin destruction and anaphase progression in meiosis I and II in Drosophila. *Dev. Camb. Engl.* **134,** 891–899 (2007).

25. Martin, A. *et al.* Diversification of complex butterfly wing patterns by repeated regulatory evolution of a Wnt ligand. *Proc. Natl. Acad. Sci.* **109,** 12632–12637 (2012).
26. Koch, P. B., Lorenz, U., Brakefield, P. M. & ffrench-Constant, R. H. Butterfly wing pattern mutants: developmental heterochrony and co-ordinately regulated phenotypes. *Dev. Genes Evol.* **210,** 536–544 (2000).
27. Gilbert, L. E., Forrest, H. S., Schultz, T. D. & Harvey, D. J. Correlations of ultrastructure and pigmentation suggest how genes control development of wing scales of Heliconius butterflies. *J. Res. Lepidoptera* **26,** 141–160 (1988).
28. Mallet, J. & Barton, N. H. Strong Natural Selection in a Warning-Color Hybrid Zone. *Evolution* **43,** 421–431 (1989).
29. Wahlberg, N., Wheat, C. W. & Peña, C. Timing and Patterns in the Taxonomic Diversification of Lepidoptera (Butterflies and Moths). *PLoS ONE* **8,** e80875 (2013).
30. Surridge, A. *et al.* Characterisation and expression of microRNAs in developing wings of the neotropical butterfly Heliconius melpomene. *BMC Genomics* **12,** 62 (2011).

Supplementary Information is linked to the online version of the paper at www.nature.com/nature.

Acknowledgements We thank Christopher Saski, Clemson University, for assembly of the *He* BACs. Moises Abanto and Adriana Tapia assisted with raising butterflies. Thanks to Mathieu Chouteau, Jake Morris and Kanchon Dasmahapatra for providing larvae for *in situ* hybridisations. Anna Morrison, Robert Tetley, Sarah Carl and Hanna Wegener assisted with lab work at the University of Cambridge. Simon Baxter made the *Hm* fosmid libraries. We thank the governments of Colombia, Ecuador, Panama and Peru for permission to collect butterflies. This work was funded by a Leverhulme Trust award and BBSRC grant (H01439X/1) to CDJ, NSF grants (DEB 1257689, IOS 1052541) to WOM, an ERC starting

250 grant to MJ and a French National Agency for Research (ANR) grant to VL (ANR-13-JSV7-
251 0003-01). NJN is funded by a NERC fellowship (NE/K008498/1).

252

253 **Author Contributions** NJN performed the association analyses, 5' RACE, RT-PCR, qRT-
254 PCR and prepared the manuscript. NJN and CDJ co-ordinated the research. CP-D performed
255 and analysed the microarray and RNAseq experiments. AW performed the *Hn* association
256 analysis. MS assembled and annotated the *HeCr* BAC reference and the *He* alignments. SVS
257 performed *in situ* hybridizations. RWRW performed the transgenic experiments and analysis
258 of *de novo* assembled sequences and fosmids together with JJH. GW and LF initially
259 identified splicing variants of *cortex*. LM performed crosses between *Hm* races. HH screened
260 the *HeCr* BAC library. CS and RM provided samples. AD contributed to the *Hm* BAC
261 sequencing and annotation. R-fC, MJ, VL, WOM and CDJ are PIs who obtained funding and
262 led the project elements. All authors commented on the manuscript.

263

264 **Author Information** Short read sequence data generated for this study are available from
265 ENA (http://www.ebi.ac.uk/ena) under study accession PRJEB8011 and PRJEB12740 (see
266 Supplementary Table 1 for previously published data accessions). The updated Cr contig is
267 deposited in Genbank with accession KC469893. The assembled *Hm* fosmid sequences are
268 deposited in Genbank with accessions KU514430-KU514438. The microarray data are
269 deposited in GEO with accessions GSM1563402- GSM1563497. Reprints and permissions
270 information is available at www.nature.com/reprints. Correspondence and requests for
271 materials should be addressed to n.nadeau@sheffield.ac.uk or c.jiggins@zoo.cam.ac.uk

272

273

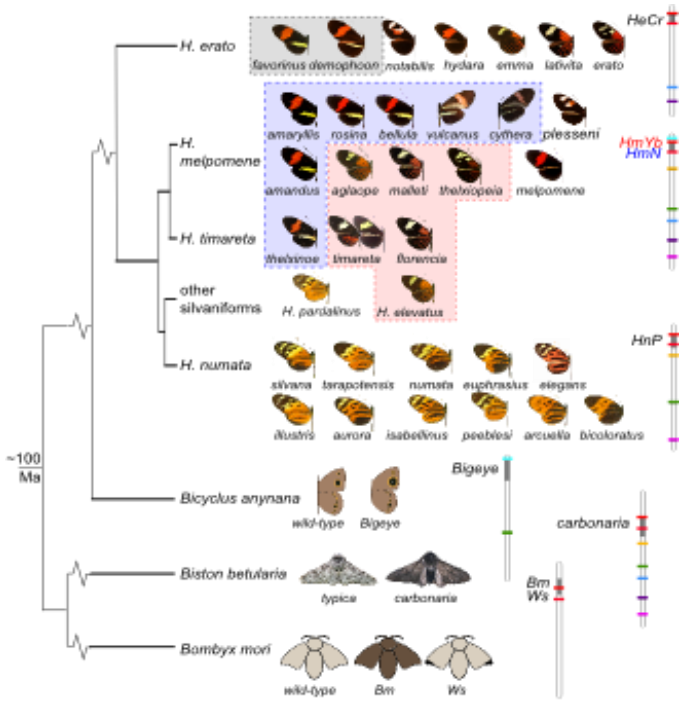

Figure 1. A homologous genomic region controls a diversity of phenotypes across the Lepidoptera. Left: phylogenetic relationships[29]. Right: chromosome maps with colour pattern intervals in grey, coloured bars represent markers used to assign homology[5,8–10], the first and last genes from Fig 2 shown in red. In *He* the *HeCr* locus controls the yellow hind-wing bar phenotype (grey boxed races). In *Hm* it controls both the yellow hind-wing bar (*HmYb*, pink box) and the yellow forewing band (*HmN*, blue box). In *Hn* it modulates black, yellow and orange elements on both wings (*HnP*), producing phenotypes that mimic butterflies in the genus *Melinaea*. Morphs/races of *Heliconius* species included in this study are shown with names.

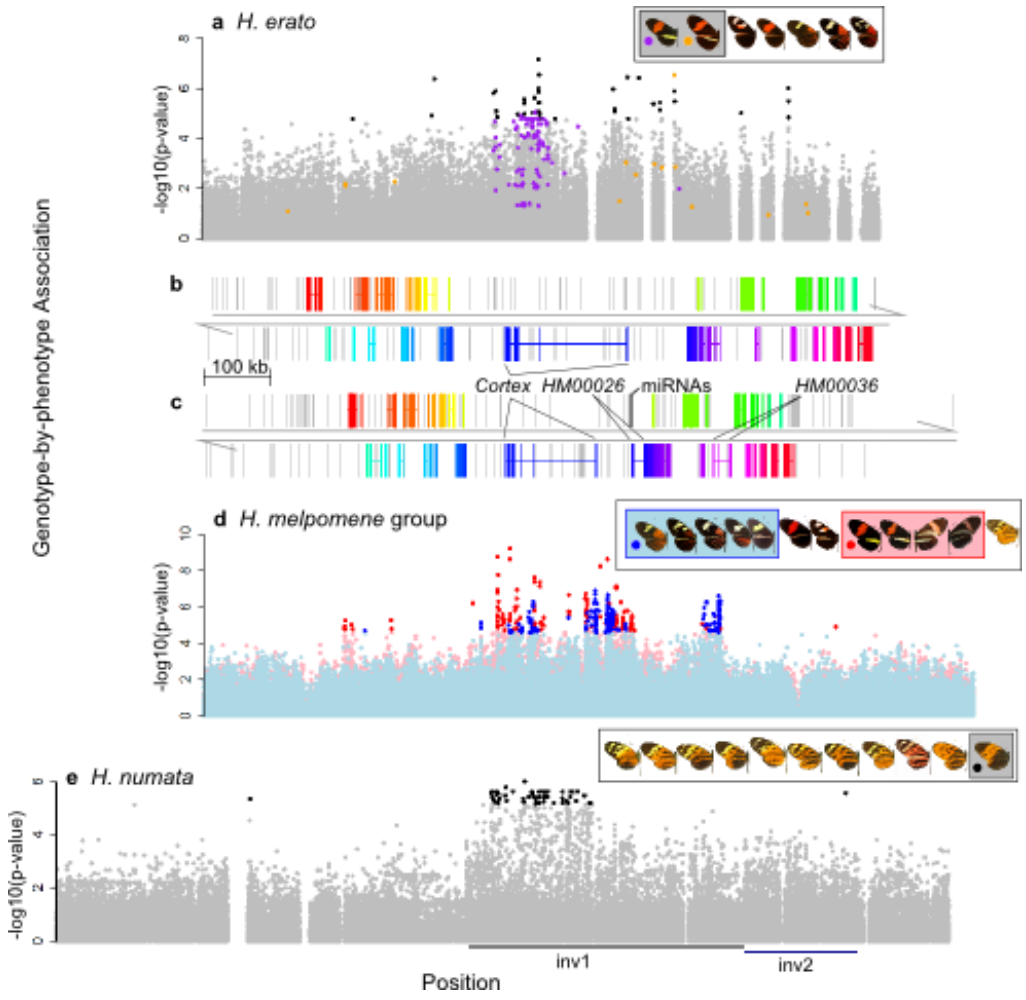

Figure 2. Association analyses across the genomic region known to contain major colour pattern loci in *Heliconius*. A) Association in *He* with the yellow hind-wing bar (n=45). Coloured SNPs are fixed for a unique state in *He demophoon* (orange) or *He favorinus* (purple). B) Genes in *He* with direct homologs in *Hm*. Genes are in different colours with exons (coding and UTRs) connected by a line. Grey bars are transposable elements. C) *Hm* genes and transposable elements: colours correspond to homologous *He* genes; MicroRNAs[30] in black. D) Association in the *Hm/timareta*/silvaniform group with the yellow hind-wing bar (red) and yellow forewing band (blue) (n=49). E) Association in *Hn* with the *bicoloratus* morph (n=26); inversion positions[13] shown below. In all cases black/dark coloured points are above the strongest associations found outside the colour pattern scaffolds (*He* p=1.63e-05; *Hm* p=2.03e-05 and p=2.58e-05; *Hn* p=6.81e-06).

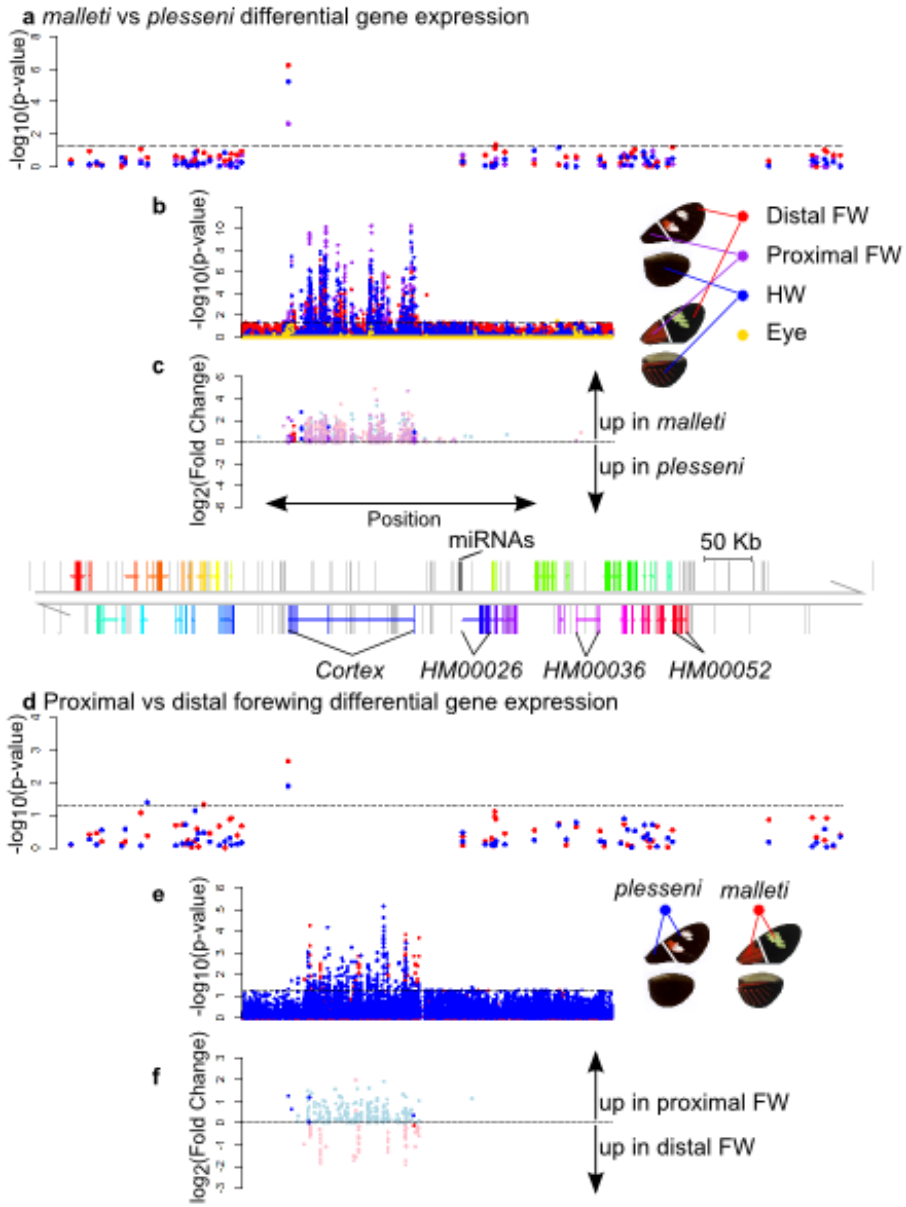

296

297 Figure 3. Differential gene expression across the genomic region known to contain major
298 colour pattern loci in *Heliconius melpomene*. Expression differences in day 3 pupae, for all
299 genes in the *Yb* interval (A,D) and tiling probes spanning the central portion of the interval
300 (B,C,E,F). Expression is compared between races for each wing region (A,B,C) and between
301 proximal and distal forewing sections for each race (D,E,F). C and F: magnitude and
302 direction of expression difference ($\log_2$ fold-change) for tiling probes showing significant
303 differences ($p \leq 0.05$); probes in known *cortex* exons shown in dark colours. Gene *HM00052*

304 was differentially expressed between other races in RNA sequence data (Supplementary
305 Information) but is not differentially expressed here.

306

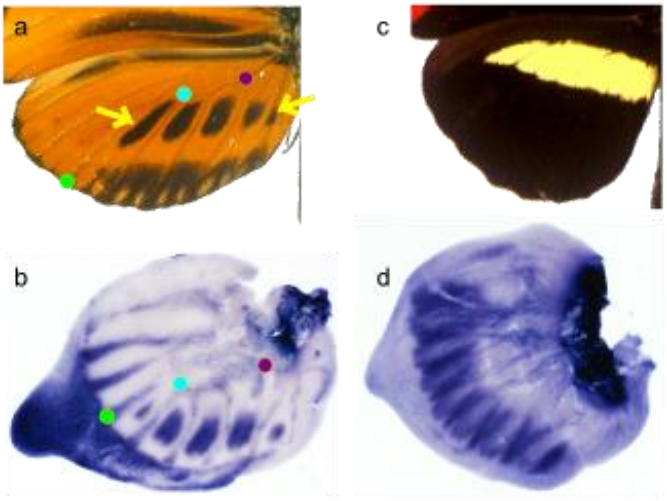

307

308 Figure 4. *In situ* hybridisations of *cortex* in hind-wings of final instar larvae. B) *Hn*
309 *tarapotensis*; adult wing shown in A, coloured points indicate landmarks, yellow arrows
310 highlight adult pattern elements corresponding to the *cortex* staining. D) *Hm rosina*; adult
311 wing shown in C, staining patterns in other *Hm* races (*meriana* and *aglaope*) appeared
312 similar. The probe used was complementary to the *cortex* isoform with the longest open
313 reading frame (also the most common, Supplementary Information).

314

315 **Methods**

316 ***He Cr reference***

317 *Cr* is the homologue of *Yb* in *He* (Fig 1). An existing reference for this region was available
318 in 3 pieces (467,734bp, 114,741bp and 161,149bp, GenBank: KC469893.1)[31]. We screened
319 the same BAC library used previously[11,31] using described procedures[11] with probes designed

to the ends of the existing BAC sequences and the *HmYb* BAC reference sequence. Two BACs (04B01 and 10B14) were identified as spanning one of the gaps and sequenced using Illumina 2x250 bp paired-end reads collected on the Illumina MiSeq. The raw reads were screened to remove vector and *E.* coli bases. The first 50k read pairs were taken for each BAC and assembled individually with the Phrap[32] software and manually edited with consed[33]. Contigs with discordant read pairs were manually broken and properly merged using concordant read data. Gaps between contig ends were filled using an in-house finishing technique where the terminal 200bp of the contig ends were extracted and queried against the unused read data for spanning pairs, which were added using the addSolexaReads.perl script in the consed package. Finally, a single reference contig was generated by identifying and merging overlapping regions of the two consensus BAC sequences.

In order to fill the remaining gap (between positions 800,387 and 848,446) we used the overhanging ends to search the scaffolds from a preliminary *He* genome assembly of five Illumina paired end libraries with different insert sizes (250, 500, 800, 4300 and 6500bp) from two related *He demophoon* individuals. We identified two scaffolds (scf1869 and scf1510) that overlapped and spanned the gap (using 12,257bp of the first scaffold and 35,803bp of the second).

The final contig was 1,009,595bp in length of which 2,281bp were unknown (N's). The *HeCr* assembly was verified by aligning to the *HmYb* genome scaffold (HE667780) with mummer and blast. The *HeCr* contig was annotated as described previously[32], with some minor modifications. Briefly this involved first generating a reference based transcriptome assembly with existing *H. erato* RNA-seq wing tissue (GenBank accession SRA060220). We used Trimmomatic[34] (v0.22), and FLASh[35] (v1.2.2) to prepare the raw sequencing reads, checking the quality with FastQC[36] (v0.10.0). We then used the Bowtie/TopHat/Cufflinks[37–39] pipeline

to generate transcripts for the unmasked reference sequence. We generated gene predictions with the MAKER pipeline[40] (v2.31). Homology and synteny in gene content with the *Hm Yb* reference were identified by aligning the *Hm* coding sequences to the *He* reference with BLAST. Homologous genes were present in the same order and orientation in *He* and *Hm* (Fig 2B,C). Annotations were manually adjusted if genes had clearly been merged or split in comparison to *H. melpomene* (which has been extensively manually curated[12]). In addition *He cortex* was manually curated from the RNA-seq data and using *Exonerate*[41] alignments of the *H. melpomene* protein and mRNA transcripts, including the 5' UTRs.

Genotype-by-phenotype association analyses

Information on the individuals used and ENA accessions for sequence data are given in Supplementary Table 1. We used shotgun Illumina sequence reads from 45 *He* individuals from 7 races that were generated as part of a previous study[31] (Supplementary Information). Reads were aligned to an *He* reference containing the *Cr* contig and other sequenced *He* BACs[11,31] with BWA[42] , which has previously been found to work better than Stampy[43] (which was used for the alignments in the other species) with an incomplete reference sequence[31]. The parameters used were as follows: Maximum edit distance (n), 8; maximum number of gap opens (o), 2; maximum number of gap extensions (e), 3; seed (l), 35; maximum edit distance in seed (k), 2. We then used Picard tools to remove PCR and optical duplicate sequence reads and GATK[44] to re-align indels and call SNPs using all individuals as a single population. Expected heterozygosity was set to 0.2 in GATK. 132,397 SNPs were present across *Cr*. A further 52,698 SNPs not linked to colour pattern loci were used to establish background association levels.

For the *Hm / Hn* clade we used previously published sequence data from 19 individuals from enrichment sequencing targeting of the *Yb* region, the unlinked *HmB/D* region that controls

the presence/absence of red colour pattern elements, and ~1.8Mb of non-colour pattern genomic regions[45], as well as 9 whole genome shotgun sequenced individuals[18,46]. We added targeted sequencing and shotgun whole genome sequencing of an additional 47 individuals (Supplementary Information). Alignments were performed using Stampy[43] with default parameters except for substitution rate which was set to 0.01. We again removed duplicates and used GATK to re-align indels and call SNPs with expected heterozygosity set to 0.1.

The analysis of the *Hm/timareta*/silvaniform included 49 individuals, which were aligned to v1.1 of the *Hm* reference genome with the scaffolds containing *Yb* and *HmB/D* swapped with reference BAC sequences[18], which contained fewer gaps of unknown sequence than the genome scaffolds. 232,631 SNPs were present in the *Yb* region and a further 370,079 SNPs were used to establish background association levels.

The *Hn* analysis included 26 individuals aligned to unaltered v1.1 of the *Hm* reference genome, because the genome scaffold containing *Yb* is longer than the BAC reference making it easier to compare the inverted and non-inverted regions present in this species. We tested for associations at 262,137 SNPs on the *Yb* scaffold with the *Hn bicoloratus* morph, which had a sample of 5 individuals.

We measured associations between genotype and phenotype using a score test (qtscore) in the GenABEL package in R[47]. This was corrected for background population structure using a test specific inflation factor, λ, calculated from the SNPs unlinked to the major colour pattern controlling loci (described above), as the colour pattern loci are known to have different population structure to the rest of the genome[14,15,18]. We used a custom perl script to convert GATK vcf files to Illumina SNP format for input to genABEL[47]. genABEL does not accept multiallelic sites, so the script also converted the genotype of any individuals for which a third (or fourth) allele was present to a missing genotype (with these defined as the lowest

393 frequency alleles). Custom R scripts were used to identify sites showing perfect associations
394 with calls for >75% of individuals.

395 ***Microarray Gene Expression Analyses***

396 We designed a Roche NimbleGen microarray (12x135K format) with probes for all annotated
397 *Hm* genes[18] and tiling the central portion of the *Yb* BAC sequence contig that was previously
398 identified as showing the strongest differentiation between *Hm* races[45]. In addition to the
399 *HmYb* tilling array probes there were 6,560 probes tiling *HmAc* (a third unlinked colour
400 pattern locus) and 10,716 probes tiling *HmB/D*, again distanced on average at 10bp intervals.
401 The whole-genome gene expression array contained 107,898 probes in total.

402 This was interrogated with Cy3 labelled double stranded cDNA generated from total RNA
403 (with a SuperScript double-stranded cDNA synthesis kit, Invitrogen, and a one-colour DNA
404 labelling kit, Niblegen) from four pupal developmental stages of *Hm plesseni* and *malleti.*
405 Pupae were from captive stocks maintained in insectary facilities in Gamboa, Panama. Tissue
406 was stored in RNA later at -80°C prior to RNA extraction. RNA was extracted using TRIzol
407 (Invitrogen) followed by purification with RNeasy (Qiagen) and DNase treated with DNA-
408 free (Ambion). Quantification was performed using a Qubit 2.0 fluorometer (Invitrogen) and
409 purity and integrity assessed using a Bioanalyzer 2100 (Agilent). Samples were randomised
410 and each hybridised to a separate array. The *HmYb* probe array contained 9,979 probes
411 distanced on average at 10bp. The whole-genome expression array contained on average 9
412 probes per annotated gene in the genome (v1.1[18]) as well as any transcripts not annotated but
413 predicted from RNA-seq evidence.

414 Background corrected expression values for each probe were extracted using NimbleScan
415 software (version 2.3). Analyses were performed with the LIMMA package implemented in
416 R/Bioconductor[48]. The tiling array and whole-genome data sets were analysed separately.

Expression values were extracted and quantile-normalised, $\log_2$-transformed, quality controlled and analysed for differences in expression between individuals and wing regions. P-values were adjusted for multiple hypotheses testing using the False Discovery Rate (FDR) method [49].

In situ hybridisations

Hn and *Hm* larvae were reared in a greenhouse at 25-30˚C and sampled at the last instar. In situ hybridizations were performed according to previously described methods[25] with a *cortex* riboprobe synthesized from a 831-bp cDNA amplicon from *Hn*. Wing discs were incubated in a standard hybridization buffer containing the probe for 20-24 h at 60°C. For secondary detection of the probe, wing discs were incubated in a 1:3000 dilution of anti-digoxigenin alkaline phosphatase Fab fragments and stained with BM Purple for 3-6 h at room temperature. Stained wing discs were photographed with a Leica DFC420 digital camera mounted on a Leica Z6 APO stereomicroscope.

De novo assembly of short read data in Hm and related taxa

In order to better characterise indel variation from the short-read sequence data used for the genotype-by-phenotype association analysis, we performed *de novo* assemblies of a subset of *Hm* individuals and related taxa with a diversity of phenotypes (Extended Data Figure 2). Assemblies were performed using the *de novo* assembly function of CLCGenomics Workbench v.6.0 under default parameters. The assembled contigs were then BLASTed against the *Yb* region of the *Hm melpomene* genome[18], using Geneious v.8.0. The contigs identified by BLAST were then concatenated to generate an allele sequence for each individual. Occasionally two unphased alleles were generated when two contigs were matched to a given region. If more than two contigs of equal length matched then this was

considered an unresolvable repeat region and replaced with Ns. The assembled alleles were then aligned using the MAFFT alignment plugin in Geneious v.8.0.

Long-range PCR targeted sequencing of cortex in Hm aglaope and Hm amaryllis

We generated two long-range PCR products covering 88.8% of the 1,344bp coding region of *cortex* (excluding 67bp at the 5' end and 83bp at the 3' end, further details in Supplementary Information). A product spanning coding exons 5 to 9 (the final exon) was obtained from 29 *Hm amaryllis* individuals and 29 *Hm aglaope* individuals; a product spanning coding exons 2 to 5 was obtained from 32 *Hm amaryllis* individuals and 14 *Hm aglaope*. In addition, a product spanning exons 4 to 6 was obtained from 6 *Hm amaryllis* and 5 *Hm aglaope* that failed to amplify one or both of the larger products. Long-range PCR was performed using Extensor long-range PCR mastermix (Thermo Scientific) following manufacturers guidelines with a 60˚C annealing temperature in a 10-20µl volume. The product spanning coding exons 5 to 9 was obtained with primers HM25_long_F1 and HM25_long_R4 (see Supplementary Table 2 for primer sequences); the product spanning coding exons 2 to 5 was obtained with primers HM25_long_F4 and HM25_long_R2; the product spanning exons 4 to 6 was obtained with primers 25_ex5-ex7_r1 and 25_ex5-ex7_f1. Products were pooled for each individual, including 5 additional products from the *Yb* locus and 7 products in the region of the *HmB/D* locus. They were then cleaned using QIAquick PCR purification kit (QIAgen) before being quantified with a Qubit Fluorometer (Life Technologies) and pooled in equimolar amounts for each individual, taking into account variation in the length and number of PCR products included for each individual (because of some PCR failures, ie. proportionally less DNA was included if some PCR products were absent for a given individual).

Products were pooled within individuals (including additional products for other genes not analysed here) and then quantified and pooled in equimolar amounts for each individual within each race. The pooled products for each race (*Hm aglaope* and *amaryllis)* were then prepared as two separate libraries with molecular identifiers and sequenced on a single lane of an Illumina GAIIx. Analysis was performed using Galaxy and the history is available at https://usegalaxy.org/u/njnadeau/h/long-pcr-final. Reads were quality filtered with a minimum quality of 20 required over 90% of the read, which resulted in 5% of reads being discarded. Reads were then quality trimmed to remove bases with quality less than 20 from the ends. They were then aligned to the target regions using the fosmid sequences from known races[45] with sequence from the *Yb* BAC walk[12] used to fill any gaps. Alignments were performed with BWA v0.5.6[42] and converted to pileup format using Samtools v0.1.12 before being filtered based on quality (≥20) and coverage (≥10). BWA alignment parameters were as follows: fraction of missing alignments given 2% uniform base error rate (aln -n) 0.01; maximum number of gap opens (aln -o) 2; maximum number of gap extensions (aln -e) 12; disallow long deletion within 12 bp towards the 3'-end (aln -d); number of first subsequences to take as seed (aln -l) 100. We then calculated coverage and minor allele frequencies for each race and the difference between these using custom scripts in R[50].

Sequencing and analysis of Hm fosmid clones

Fosmid libraries had previously been made from single individuals of 3 *Hm* races (*rosina, amaryllis* and *aglaope*) and several clones overlapping the *Yb* interval had been sequenced[45]. We extended the sequencing of this region, particularly the region overlapping *cortex* by sequencing an additional 4 clones from *Hm rosina* (1051_83D21, accession KU514430; 1051_97A3, accession KU514431; 1051_65N6, accession KU514432; 1051_93D23, accession KU514433) 2 clones from *Hm amaryllis* (1051_13K4, accession KU514434; 1049_8P23, accession KU514435) and 3 clones from *Hm aglaope* (1048_80B22, accession

KU514437; 1049_19P15, accession KU514436; 1048_96A7, accession KU514438). These were sequenced on a MiSeq 2000, and assembled using the *de novo* assembly function of CLCGenomcs Workbench v.6.0. The individual clones (including existing clones 1051-143B3, accession FP578990; 1049-27G11, accession FP700055; 1048-62H20, accession FP565804) were then aligned to the BAC and genome scaffold[18] references using the MAFFT alignment plugin of Geneious v.8.0. Regions of general sequence similarity were identified and visualised using MAUVE[51]. We merged overlapping clones from the same individual if they showed no sequence differences, indicating that they came from the same allele. We identified transposable elements (TEs) using nBLAST with an insect TE list downloaded from Repbase Update[52] including known *Heliconius* specific TEs[53].

5' RACE, RT-PCR and qRT-PCR

All tissues used for gene expression analyses were dissected from individuals from captive stocks derived from wild caught individuals of various races of *Hm (aglaope, amaryllis, melpomene, rosina, plesseni, malleti*) and F2 individuals from a *Hm rosina* (female) x *Hm melpomene* (male) cross. Experimental individuals were reared at 28°C-31°C. Developing wings were dissected and stored in RNAlater (Ambion Life Technologies). RNA was extracted using a QIAgen RNeasy Mini kit following the manufacturer's guidelines and treated with TURBO DNA-free DNase kit (Ambion Life Technologies) to remove remaining genomic DNA. RNA quantification was performed with a Nanodrop spectrophotometer, and the RNA integrity was assessed using the Bioanalyzer 2100 system (Agilent).

Total RNA was thoroughly checked for DNA contamination by performing PCR for EF1α (using primers ef1-a_RT_for and ef1-a_RT_rev, Table S2) with 0.5µl of RNA extract (50ng-1µg of RNA) in a 20µl reaction using a polymerase enzyme that is not functional with RNA

template (BioScript, Bioline Reagents Ltd.). If a product amplified within 45 cycles then the RNA sample was re-treated with DNase.

Single stranded cDNA was synthesised using BioScript MMLV Reverse Transcriptase (Bioline Reagents Ltd.) with random hexamer (N6) primers and 1µg of template RNA from each sample in a 20 µl reaction volume following the manufacturer's protocol. The resulting cDNA samples were then diluted 1:1 with nuclease free water and stored at -80˚C.

5' RACE was performed using RNA from hind-wing discs from one *Hm aglaope* and one *Hm amaryllis* final instar larvae with a SMARTer RACE kit from Clonetech (California, USA). The gene specific primer used for the first round of amplification was anchored in exon 4 (fzl_raceex5_R1, Supplementary Table 2). Secondary PCR of these products was then performed using a primer in exon 2 (HM25_long_F2, Supplementary Table 2) and the nested universal primer A. Other isoforms were detected by RT-PCR using primers within exons 2 and 9 (gene25_for_full1 and gene25_rev_ex3). We identified isoforms from 5' RACE and RT-PCR products by cutting individual bands from agarose gels and if necessary by cloning products before Sanger sequencing. Cloning of products was performed using TOPO TA (Invitrogen) or pGEM-T (Promega) cloning kits. Sanger sequencing was performed using BigDye terminator v3.1 (Applied Biosystems) run on an ABI13730 capillary sequencer. Primers fzl_ex1a_F1 and fzl_ex4_R1 were used to confirm expression of the furthest 5' UTR. For isoforms that appeared to show some degree of race specificity we designed isoform specific PCR primers spanning specific exon junctions (Extended Data Fig 2, 4, Supplementary Table 2) and used these to either qualitatively (RT-PCR) or quantitatively (qRT-PCR) assess differences in expression between races.

We performed qRT-PCR using SensiMix SYBR green (Bioline Reagents Ltd.) with 0.2-0.25µM of each primer and 1µl of the diluted product from the cDNA reactions. Reactions

were performed in an Opticon 2 DNA engine (MJ Research), with the following cycling parameters: 95˚C for 10min, 35-50 x: (95˚C for 15sec, 55-60˚C for 30sec, 72˚ for 30sec), 72˚C for 5min. Melting curves were generated between 55˚C and 90˚C with readings taken every 0.2˚C for each of the products to check that a single product was generated. At least one product from each set of primers was also run on a 1% agarose gel to check that a single product of the expected size was produced and the identity of the product confirmed by direct sequencing (See Supplementary Table 2 for details of primers for each gene). We used two housekeeping genes (*EF1α* and *Ribosomal Protein S3A)* for normalisation and all results were taken as averages of triplicate PCR reactions for each sample.

C_t values were defined as the point at which fluorescence crossed a threshold (R_{Ct}) adjusted manually to be the point at which fluorescence rose above the background level. Amplification efficiencies (E) were calculated using a dilution series of clean PCR product. Starting fluorescence, which is proportional to the starting template quantity, was calculated as $R_0 = R_{Ct}\,(1+E)^{-Ct}$. Normalized values were then obtained by dividing R_0 values for the target loci by R_0 values for EF1α and RPS3A. Results from both of these controls were always very similar, therefore the results presented are normalized to the mean of EF1α and RPS3A. All results were taken as averages of triplicate PCR reactions. If one of the triplicate values was more than one cycle away from the mean then this replicate was excluded. Similarly any individuals that were more than two standard deviations away from the mean of all individuals for the target or normalization genes were excluded (these are not included in the numbers of individuals reported). Statistical significance was assessed by Wilcoxon rank sum tests performed in R[50].

RNAseq analysis of Hm amaryllis/aglaope

RNA-seq data for hind-wings from three developmental stages had previously been obtained for two individuals of each race at each stage (12 individuals in total) and used in the annotation of the *Hm* genome[18] (deposited in ENA under study accessions ERP000993 and PRJEB7951). Four samples were multiplexed on each sequencing lane with the fifth instar larval and day 2 pupal samples sequenced on a GAIIx sequencer and the day 3 pupal wings sequenced on a Hiseq 2000 sequencer.

Two methods were used for alignment of reads to the reference genome and inferring read counts, Stampy[43] and RSEM (RNAseq by Expectation Maximisation)[54]. In addition we used two different R/Bioconductor packages for estimation of differential gene expression, DESeq[55] and BaySeq [56]. Read bases with quality scores < 20 were trimmed with FASTX-Toolkit (http://hannonlab.cshl.edu/fastx_toolkit/index.html). Stampy was run with default parameters except for mean insert size, which was set to 500, SD 100 and substitution rate, which was set to 0.01. Alignments were filtered to exclude reads with mapping quality <30 and sorted using Samtools[57]. We used the HT seq-count script in with HTseq[58] to infer counts per gene from the BAM files.

RSEM[54] was run with default parameters to infer a transcriptome and then map RNAseq reads against this using Bowtie[37] as an aligner. This was run with default parameters except maximum number of mismatches, which was set to 3.

Annotation and alignment of fizzy family proteins

In the arthropod genomes, some fizzy family proteins were found to be poorly annotated based on alignments to other family members. In these cases annotations were improved using well annotated proteins from other species as references in the program Exonerate[41] and the outputs were manually curated. Specifically, the annotation of *B. mori fzr* was extended based on alignment of *D. plexippus fzr*; the annotation of *B. mori fzy* was altered

582 based on alignment of *Drosophila melanogaster* and *D. plexippus fzy*; *H. melpomene fzy* was
583 identified as part of the annotated gene HMEL017486 on scaffold HE671623 (Hmel v1.1)
584 based on alignment of *D. plexippus fzy;* the *Apis mellifera fzr* annotation was altered based
585 on alignment of *D. melanogaster fzr*; the annotation of *Acyrthosiphon pisum fzr* was altered
586 based on alignment of *D. melanogaster fzr*. No one-to-one orthologues of *D. melanogaster*
587 *fzr2* were found in any of the other arthropod genera, suggesting that this gene is *Drosophila*
588 specific. Multiple sequence alignment of all the fizzy family proteins was then performed
589 using the Expresso server[59] within T-coffee[60], and this alignment was used to generate a
590 neighbour joining tree in Geneious v8.1.7.

591 **Expression of *H. melpomene cortex* in *D. melanogaster* wings**

592 *D. melanogaster* Cortex is known to generate an irregular microchaete phenotype when
593 ectopically expressed in the posterior compartment of the adult fly wing[24]. We performed the
594 same assay using *H. melpomene cortex* in order to test if this functionality was conserved.
595 Following the methods of Swan and Schüpbach[24] a UAS-GAL4 construct was created using
596 the coding region for the long isoform of *Hm cortex*, plus a *Drosophila cortex* version to act
597 as positive control. The HA-tagged *H. melpomene* UAS-*cortex* expression construct was
598 generated using cDNA reverse transcribed (Revert-Aid, Thermo-Scientific) from RNA
599 extracted (Qiagen RNeasy) from pre-ommochrome pupal wing material. An HA-tagged
600 *D.melanogaster* UAS-*cortex* version was also constructed, following the methods of Swan
601 and Schüpbach, (2007). Expression was driven by hsp70 promoter. Constructs were injected
602 into ϕC31-attP40 flies (#25709, Bloomington stock centre, Indiana; Cambridge University
603 Genetics Department, UK, fly injection service) by site directed insertion into CII via an attB
604 site in the construct. Homozygous transgenic flies were crossed with w,y';en-GAL4;UAS-
605 GFP (gift of M. Landgraf lab, Cambridge University Zoology Department) to drive

606 expression in the engrailed posterior domain of the wing, and adult offspring wings
607 photographed (Extended Data Fig 6B-D). Expression of the construct was confirmed by IHC
608 (standard *Drosophila* protocol) of final instar larval wing discs using mouse anti-HA and goat
609 anti-mouse alexa-fluor 568 secondary antibodies (Abcam), imaged by Leica SP5 confocal.
610 Successful expression of *Hm_Cortex* was confirmed by IHC against an HA tag inserted at the
611 N terminal of either protein (Extended Data Fig 6E).

612

613 **References**

614 31. Supple, M. A. *et al.* Genomic architecture of adaptive color pattern divergence and
615 convergence in Heliconius butterflies. *Genome Res.* **23,** 1248–1257 (2013).
616 32. de la Bastide, M. & McCombie, W. R. Assembling genomic DNA sequences with
617 PHRAP. *Curr. Protoc. Bioinforma. Ed. Board Andreas Baxevanis Al* **Chapter 11,**
618 Unit11.4 (2007).
619 33. Gordon, D., Abajian, C. & Green, P. Consed: a graphical tool for sequence finishing.
620 *Genome Res.* **8,** 195–202 (1998).
621 34. Bolger, A. M., Lohse, M. & Usadel, B. Trimmomatic: a flexible trimmer for Illumina
622 sequence data. *Bioinformatics* btu170 (2014). doi:10.1093/bioinformatics/btu170
623 35. Magoč, T. & Salzberg, S. L. FLASH: fast length adjustment of short reads to improve
624 genome assemblies. *Bioinformatics* **27,** 2957–2963 (2011).
625 36. Andrews, S. *FastQC*. (2011).
626 37. Langmead, B., Trapnell, C., Pop, M. & Salzberg, S. L. Ultrafast and memory-efficient
627 alignment of short DNA sequences to the human genome. *Genome Biol.* **10,** R25 (2009).
628 38. Trapnell, C., Pachter, L. & Salzberg, S. L. TopHat: discovering splice junctions with
629 RNA-Seq. *Bioinformatics* **25,** 1105–1111 (2009).

630 39. Trapnell, C. *et al.* Transcript assembly and quantification by RNA-Seq reveals
631 unannotated transcripts and isoform switching during cell differentiation. *Nat.*
632 *Biotechnol.* **28,** 511–515 (2010).
633 40. Holt, C. & Yandell, M. MAKER2: an annotation pipeline and genome-database
634 management tool for second-generation genome projects. *BMC Bioinformatics* **12,** 491
635 (2011).
636 41. Slater, G. S. & Birney, E. Automated generation of heuristics for biological sequence
637 comparison. *BMC Bioinformatics* **6,** 31 (2005).
638 42. Li, H. & Durbin, R. Fast and accurate short read alignment with Burrows-Wheeler
639 transform. *Bioinforma. Oxf. Engl.* **25,** 1754–1760 (2009).
640 43. Lunter, G. & Goodson, M. Stampy: A statistical algorithm for sensitive and fast mapping
641 of Illumina sequence reads. *Genome Res.* **21,** 936–939 (2011).
642 44. DePristo, M. A. *et al.* A framework for variation discovery and genotyping using next-
643 generation DNA sequencing data. *Nat Genet* **43,** 491–498 (2011).
644 45. Nadeau, N. J. *et al.* Genomic islands of divergence in hybridizing Heliconius butterflies
645 identified by large-scale targeted sequencing. *Philos. Trans. R. Soc. B Biol. Sci.* **367,**
646 343–353 (2012).
647 46. Martin, S. H. *et al.* Genome-wide evidence for speciation with gene flow in Heliconius
648 butterflies. *Genome Res.* **23,** 1817–1828 (2013).
649 47. Aulchenko, Y. S., Ripke, S., Isaacs, A. & van Duijn, C. M. GenABEL: an R library for
650 genome-wide association analysis. *Bioinforma. Oxf. Engl.* **23,** 1294–1296 (2007).
651 48. Smyth, G. K. in *Bioinformatics and Computational Biology Solutions Using R and*
652 *Bioconductor* (eds. Gentleman, R., Carey, V. J., Huber, W., Irizarry, R. A. & Dudoit, S.)
653 397–420 (Springer New York, 2005).

654 49. Benjamini, Y. & Hochberg, Y. Controlling the False Discovery Rate: A Practical and
655 Powerful Approach to Multiple Testing. *J. R. Stat. Soc. Ser. B Methodol.* **57,** 289–300
656 (1995).
657 50. R Development Core Team. *R: A language and environment for statistical computing*.
658 (R Foundation for Statistical Computing, 2011).
659 51. Darling, A. C. E., Mau, B., Blattner, F. R. & Perna, N. T. Mauve: Multiple Alignment of
660 Conserved Genomic Sequence With Rearrangements. *Genome Res.* **14,** 1394–1403
661 (2004).
662 52. Jurka, J. *et al.* Repbase Update, a database of eukaryotic repetitive elements. *Cytogenet.*
663 *Genome Res.* **110,** 462–467 (2005).
664 53. Lavoie, C. A., Platt, R. N., Novick, P. A., Counterman, B. A. & Ray, D. A. Transposable
665 element evolution in Heliconius suggests genome diversity within Lepidoptera. *Mob.*
666 *DNA* **4,** 21 (2013).
667 54. Li, B. & Dewey, C. N. RSEM: accurate transcript quantification from RNA-Seq data
668 with or without a reference genome. *BMC Bioinformatics* **12,** 323 (2011).
669 55. Anders, S. & Huber, W. Differential expression analysis for sequence count data.
670 *Genome Biol.* **11,** 1–12 (2010).
671 56. Hardcastle, T. J. & Kelly, K. A. baySeq: Empirical Bayesian methods for identifying
672 differential expression in sequence count data. *BMC Bioinformatics* **11,** 422 (2010).
673 57. Li, H. *et al.* The Sequence Alignment/Map format and SAMtools. *Bioinforma. Oxf. Engl.*
674 **25,** 2078–2079 (2009).
675 58. Anders, S., Pyl, P. T. & Huber, W. HTSeq - A Python framework to work with high-
676 throughput sequencing data. *bioRxiv* (2014). doi:10.1101/002824

677 59. Armougom, F. *et al.* Expresso: automatic incorporation of structural information in
678 multiple sequence alignments using 3D-Coffee. *Nucleic Acids Res.* **34,** W604–608
679 (2006).
680 60. Di Tommaso, P. *et al.* T-Coffee: a web server for the multiple sequence alignment of
681 protein and RNA sequences using structural information and homology extension.
682 *Nucleic Acids Res.* **39,** W13–17 (2011).

683

684

685 **Extended Data**

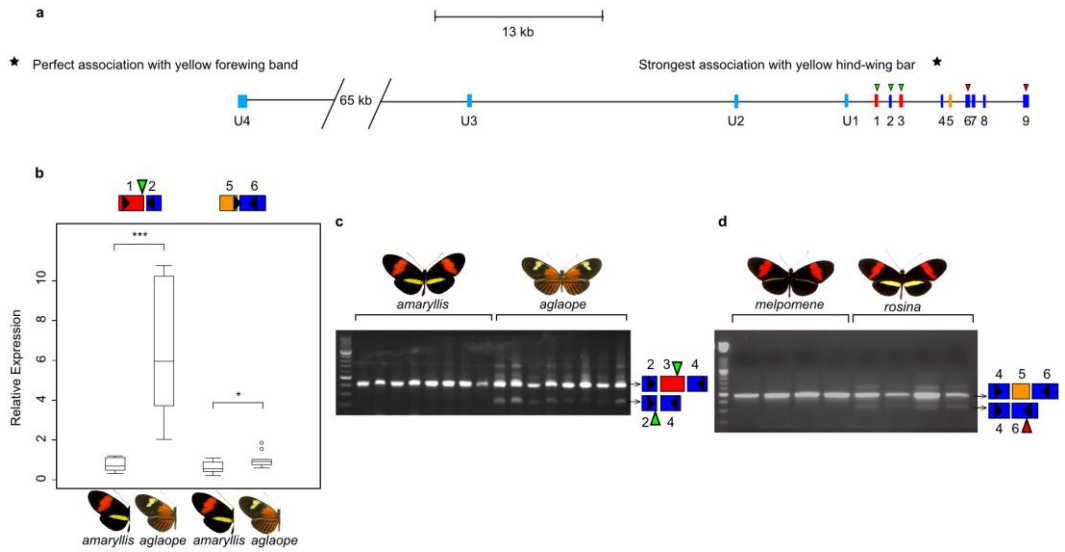

686
687 Extended Data Figure 1. A) Exons and splice variants of *cortex* in *Hm*. Orientation is
688 reversed with respect to figures 2 and 4, with transcription going from left to right. SNPs
689 showing the strongest associations with phenotype are shown with stars. B) Differential
690 expression of two regions of *cortex* between *Hm amaryllis* and *Hm aglaope* whole hindwings
691 (N=11 and N=10 respectively). Boxplots are standard (median; 75th and 25th percentiles;
692 maximum and minimum excluding outliers – shown as discrete points) C) Expression of a

693 *cortex* isoform lacking exon 3 is found in *Hm aglaope* but not *Hm amaryllis* hindwings. D)
694 Expression of an isoform lacking exon 5 is found in *Hm rosina* but not *Hm melpomene*
695 hindwings. Green triangles indicate predicted start codons and red triangles predicted stop
696 codons, with usage dependent on which exons are present in the isoform. Schematics of the
697 targeted exons are shown for each (q)RT-PCR product, black triangles indicate the position
698 of the primers used in the assay.

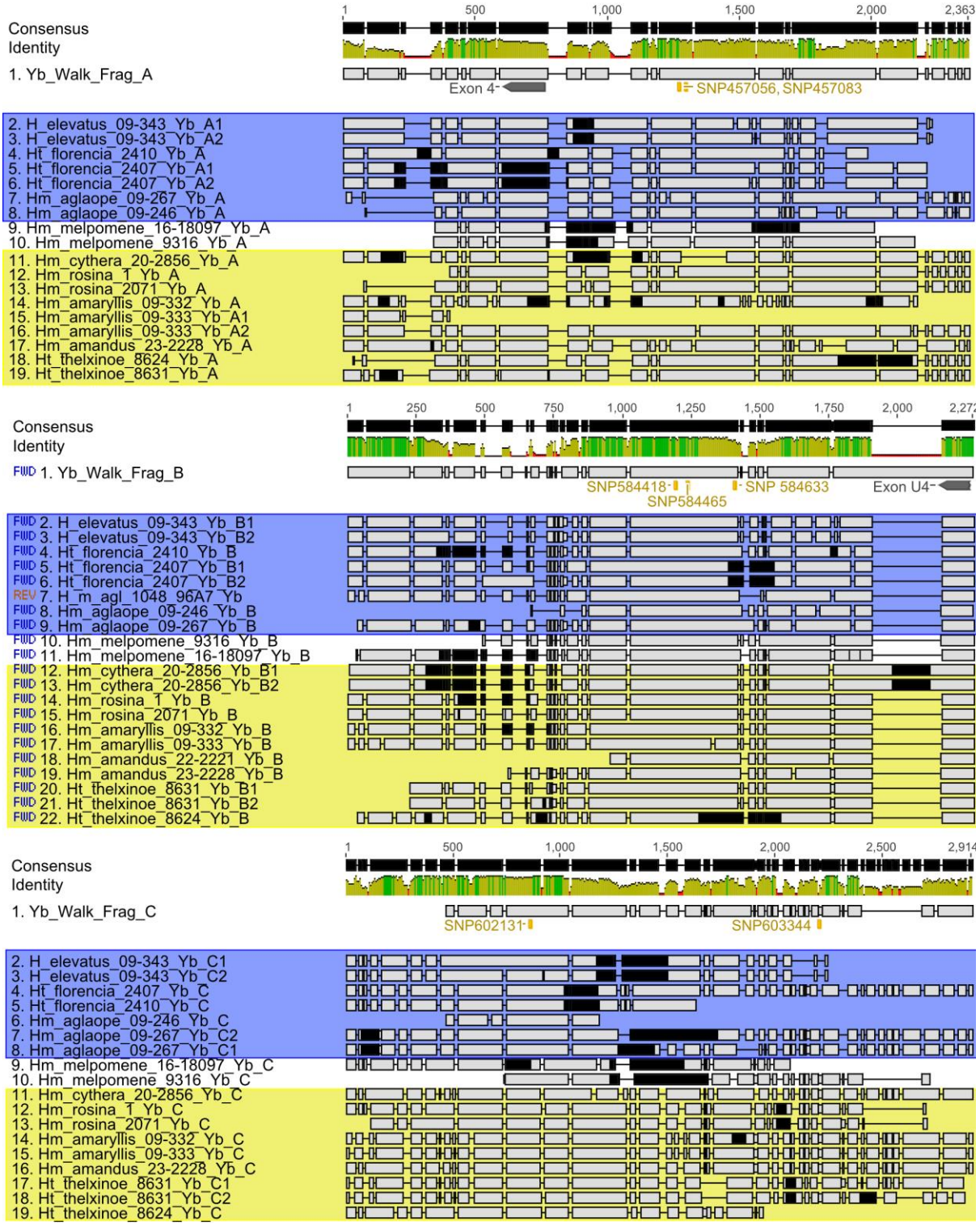

Extended Data Figure 2. Alignments of *de novo* assembled fragments containing the top associated SNPs from *Hm* and related taxa short-read data. Identified indels do not show stronger associations with phenotype that those seen at SNPs (as shown in Extended Data Table 2), although some near-perfect associations are seen in fragment C. Black regions =

missing data; yellow box = individuals with a hindwing yellow bar; blue box = individuals with a yellow forewing band.

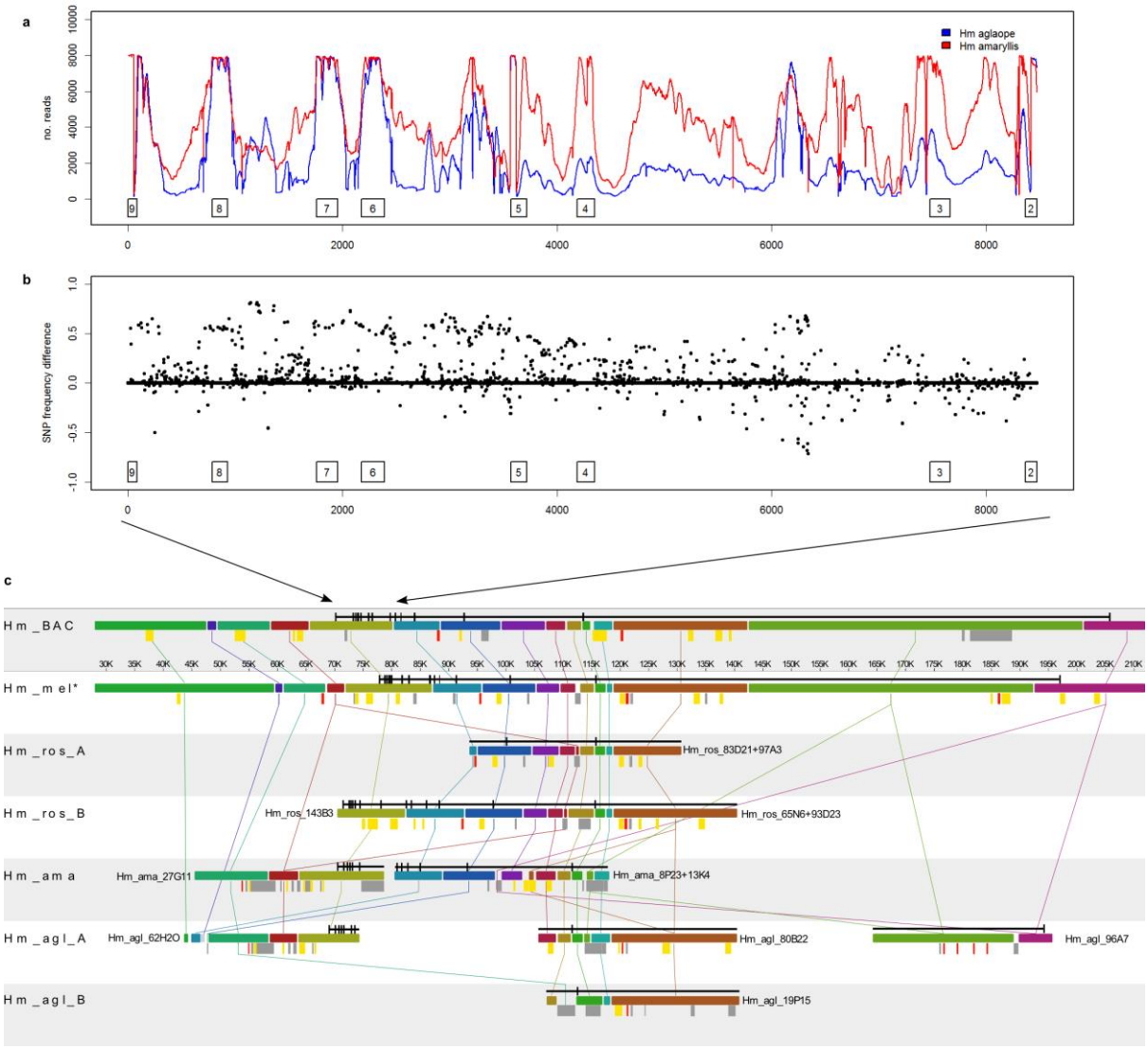

Extended Data Figure 3. Sequencing of long-range PCR products and fosmids spanning *cortex.* A) Sequence read coverage from long-range PCR products across the *cortex* coding region from 2 *Hm* races. B) Minor allele frequency difference from these reads between *Hm aglaope* and *Hm amaryllis*. Exons of *cortex* are indicated by boxes, numbered as in Extended Data Figure 2. C) Alignments of sequenced fosmids overlapping *cortex* from 3 *Hm* individuals of difference races. No major rearrangements are observed, nor any major differences in transposable element (TE) content between closely related races with different

colour patterns (*melpomene/rosina* or *amaryllis/aglaope*). *Hm amaryllis* and *rosina* have the same phenotype, but do not share any TEs that are not present in the other races. Hm_BAC = BAC reference sequence, Hm_mel = *melpomene* from new unpublished assembly of *Hm* genome[51], Hm_ros = *rosina* (2 different alleles were sequenced from this individual), Hm_ama = *amaryllis* (2 non-overlapping clones were sequenced in this individual), Hm_agla = *aglaope* (4 clones were sequenced in this individual 2 of which represent alternative alleles). Alignments were performed with Mauve: coloured bars represent homologous genomic regions. *cortex* is annotated in black above each clone. Variable TEs are shown as coloured bars below each clone: red = Metulj-like non-LTR, yellow = Helitron-like DNA, grey = other.

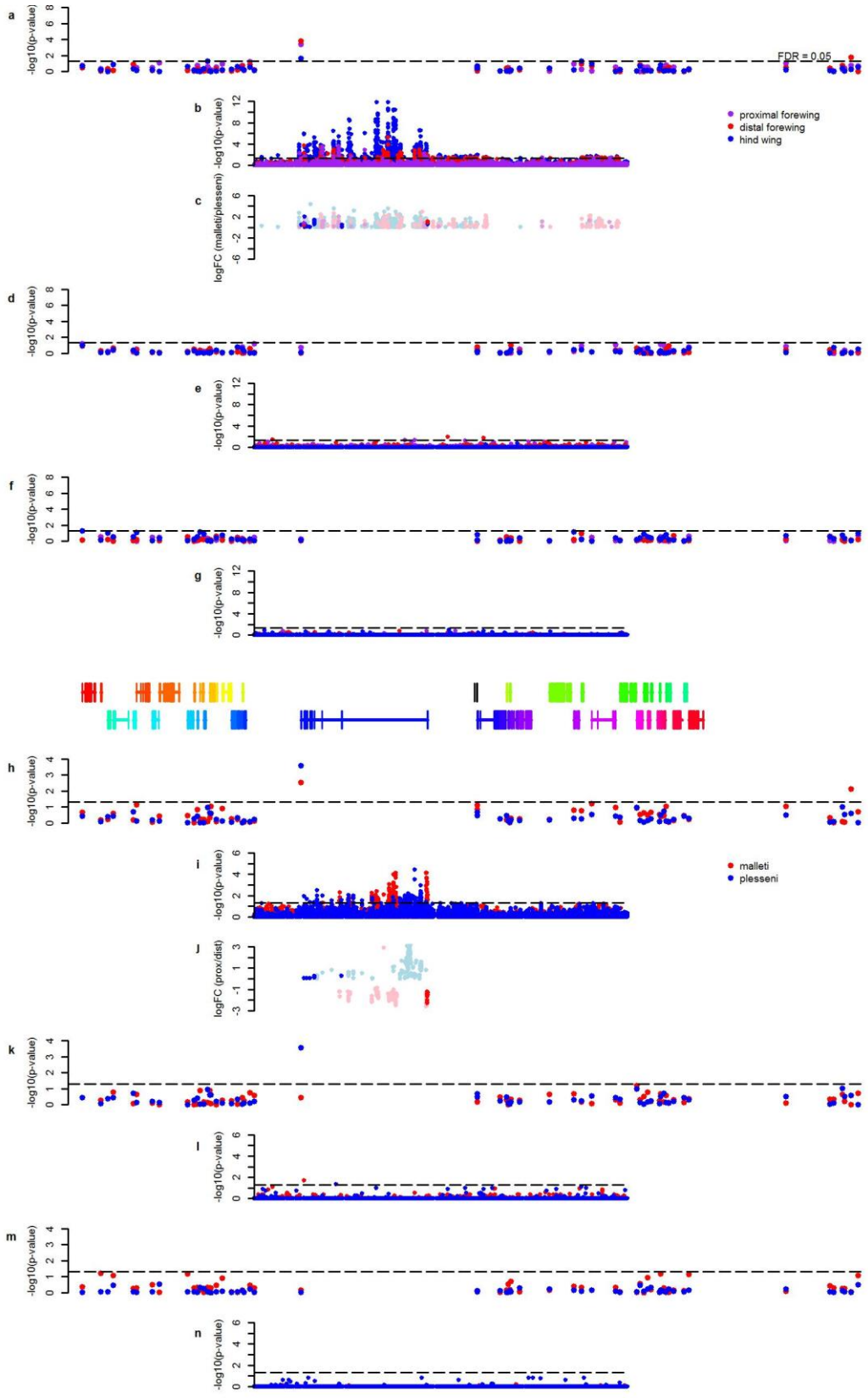

724

725 Extended Data Figure 4. Expression array results for additional stages, related to Figure 4. A-

726 G: comparisons between races (*H. m. plesseni* and *H. m. malleti*) for 3 wing regions. H-N:

comparisons between proximal and distal forewing regions for each race. Significance values (-log10(p-value)) are shown separately for genes in the *HmYb* region from the gene array (A,D,F,H,K,M) and for the *HmYb* tiling array (B,E,G,I,L,N) for day 1 (A,B,H,I), day 5 (D,E,K,L) and day 7 (F,G,M,N) after pupation. The level of expression difference (log fold change) for tiling probes showing significant differences ($p \leq 0.05$) is shown for day 1 (C and J) with probes in known *cortex* exons shown in dark colours and probes elsewhere shown as pale colours.

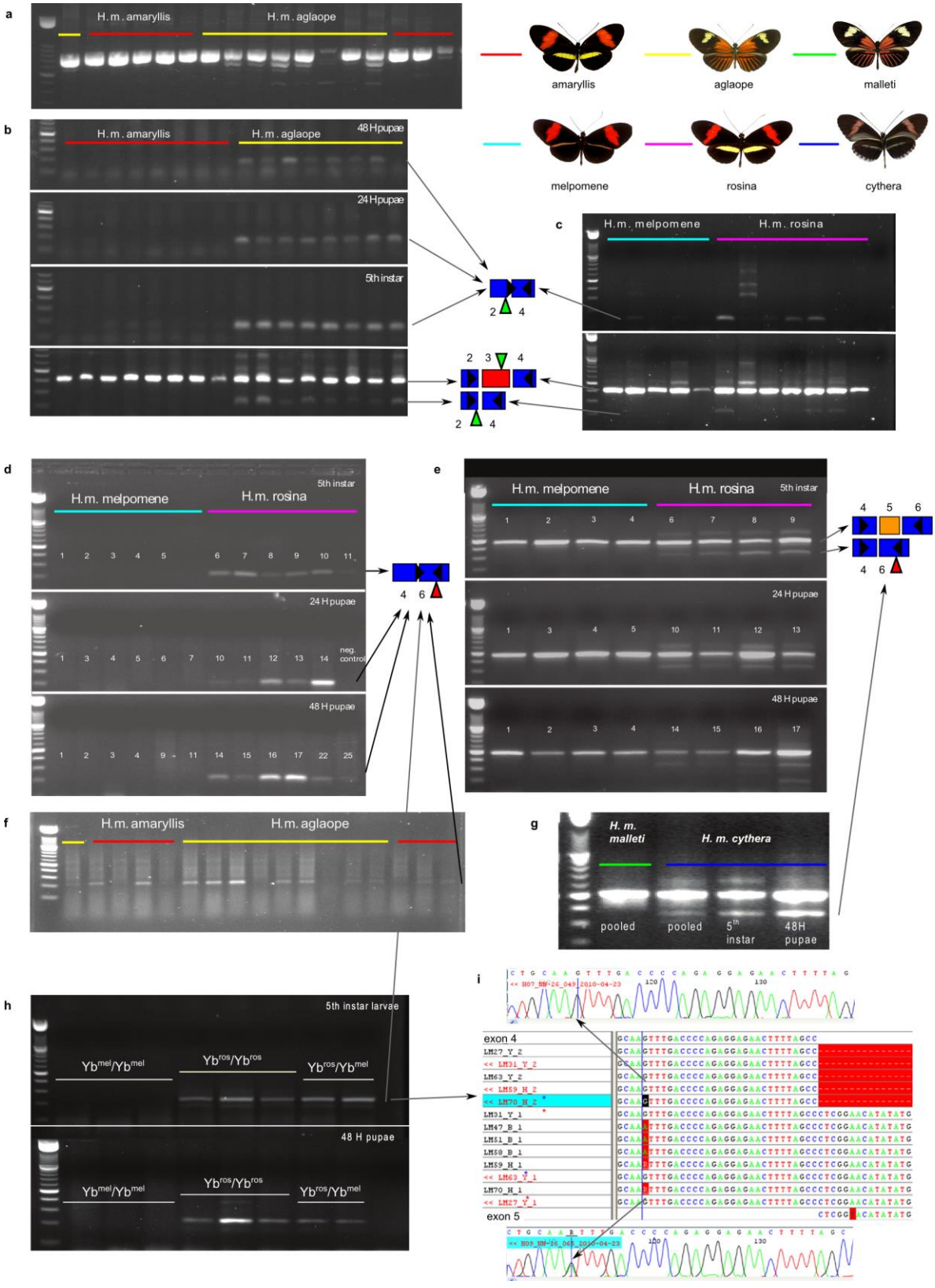

734

735 Extended Data Figure 5. Alternative splicing of *cortex*. A) Amplification of the whole *cortex*

736 coding region, showing the diversity of isoforms and variation between individuals. B)

Differences in splicing of exon 3 between *H. m. aglaope* and *H. m. amaryllis*. Products amplified with a primer spanning the exon 2/4 junction at 3 developmental stages. The lower panel shows verification of this assay by amplification between exons 2 and 4 for the same final instar larval samples (replicated in Extended Data Figure 2C) C) Lack of consistent differences between *H. m. melpomene* and *H. m. rosina* in splicing of exon 3. Top panel shows products amplified with a primer spanning the exon 2/4 junction, lower panel is the same samples amplified between exons 2 and 4. D) Differences in splicing of exon 5 between *H. m. melpomene* and *H. m. rosina*. Products amplified with a primer spanning the exon 4/6 junction at 3 developmental stages. E) Subset of samples from D amplified with primers between exons 4 and 6 for verification (middle, 24hr pupae samples are replicated in Extended Data Figure 2D). F) Lack of consistent differences between *H. m. aglaope* and *H. m. amaryllis* in splicing of exon 5. Products amplified with a primer spanning the exon 4/6 junction. G) *H. m. cythera* also expresses the isoform lacking exon 5, while a pool of 6 *H. m. malleti* individuals do not. H) Expression of the isoform lacking exon 5 from an F2 *H. m. melpomene* x *H. m. rosina* cross. Individuals homozygous or heterozygous for the *H. m. rosina HmYb* allele express the isoform while those homozygous for the *H. m. melpomene HmYb* allele do not. I) Allele specific expression of isoforms with and without exon 5. Heterozygous individuals (indicated with blue and red stars) express only the *H. m. rosina* allele in the isoform lacking exon 5 (G at highlighted position), while they express both alleles in the isoform containing exon 5 (G/A at this position).

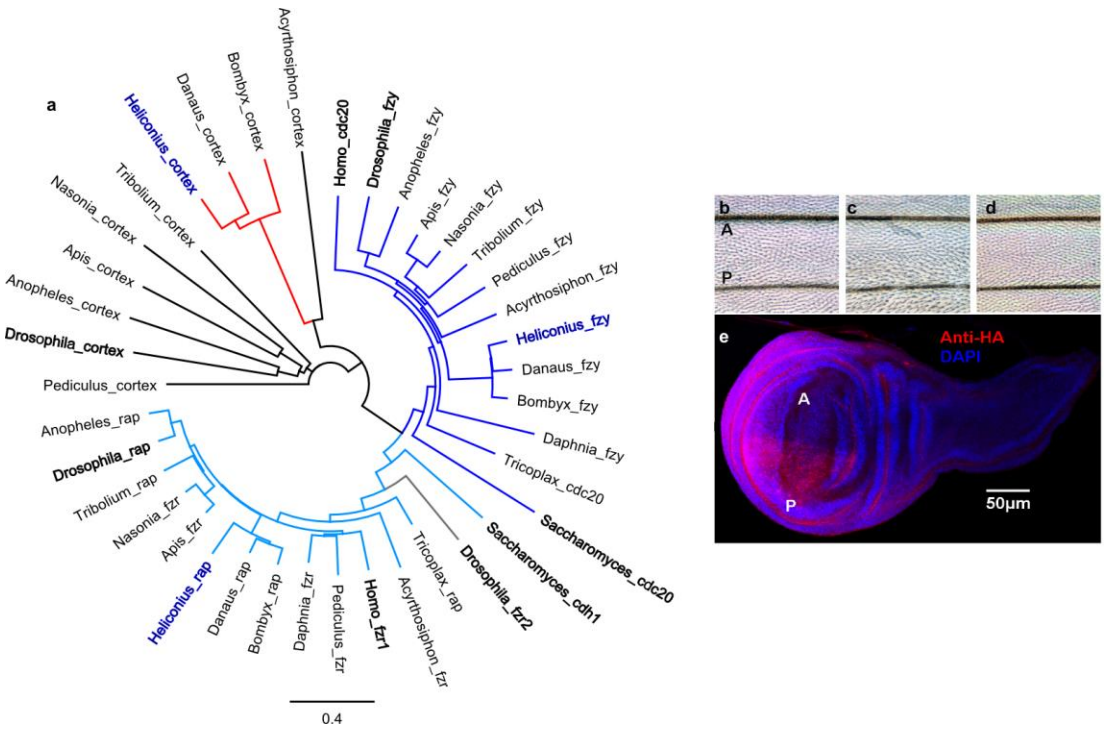

757

758 Extended Data Figure 6. Phylogeny of fizzy family proteins and effects of expressing *cortex*
759 in the Drosophila wing. A) Neighbour joining phylogeny of Fizzy family proteins including
760 functionally characterised proteins (in bold) from *Saccharomyces cerevisiae, Homo sapiens*
761 and *Drosophila melanogaster* as well as copies from the basal metazoan *Trichoplax*
762 *adhaerens* and a range of annotated arthropod genomes (*Daphnia pulex, Acyrthosiphon*
763 *pisum, Pediculus humanus, Apis mellifica, Nasonia vitripennis, Anopheles gambiae,*
764 *Tribolium castaneum*) including the lepidoptera *H. melpomene* (in blue), *Danaus plexippus*
765 and *Bombyx mori*. Branch colours: dark blue, CDC20/fzy; light blue, CDH1/fzr/rap; red,
766 lepidoptran cortex. B-E) Ectopic expression of *cortex* in *Drosophila melanogaster*.
767 *Drosophila cortex* produces an irregular microchaete phenotype when expressed in the
768 posterior compartment of the fly wing (C) whereas *Heliconius cortex* does not (D), when
769 compared to no expression (B). A, anterior; P, posterior. Successful *Heliconius cortex*
770 expression was confirmed by anti-HA IHC in the last instar *Drosophila* larva wing imaginal
771 disc (D, red), with DAPI staining in blue.

772 Extended Data Table 1. Genes in the *Yb* region and evidence for wing patterning control in

773 *Heliconius*

			Heliconius melpomene									*H. erato*			*Hn*	
Hm gene ID	*He* gene ID	Putative gene name	Yb^I	Sb^I	A^{Yb}	A^N	E^1	E^{gw}	E^{gr}	E^{tw}	E^{tr}	Cr^I	A^{pet}	A^{fav}	P^I	A^{bic}
HM00002	HERA000036	Acylpeptide hydrolase			2							x				
HM00003	HERA000037	HM00003										x				
HM00004	HERA000038	Trehalase-1B	x									x				
HM00006	HERA000038.1	Trehalase-1A	x									x				
HM00007	HERA000039	B9 protein	x									x				
HM00008	HERA000040	HM00008	x		2							x				
HM00010	HERA000041	WD40 repeat domain 85	x									x				
HM00012	HERA000042	CG2519	x					x				x				
HM00013	HERA000045	Unkempt	x									x				
HM00014	HERA000046	Histone H3	x									x				
HM00015	HERA000047	HM00015	x									x				
HM00016	HERA000048	HM00016	x									x				
HM00017	HERA000049	RecQ Helicase	x									x				
HM00018	HERA000051	HM00018	x									x				
HM00019	HERA000052	BmSuc2	x					x				x				
HM00020	HERA000053	CG5796	x									x				
HM00021	HERA000054	HM00021	x									x				
HM00022	HERA000055	Enoyl-CoA hydratase	x									x				
HM00023	HERA000056	ATP binding protein	x									x				
HM00024	HERA000057	HM00024	x									x				
HM00025	HERA000059	cortex	x	x	56	74	x	x	x	603	1796	x	2	99	x	51
HM00026	HERA000077	Poly(A)-specific ribonuclease (parn)		x	10					1	34	x			x	
HM00027	HERA000079	CG31320		x								x			x	
HM00028	HERA000080	ARP-like		x								x			x	
HM00029	HERA000081	CG4692		x								x			x	
HM00030	HERA000082	Proteasome 26S non ATPase subunit 4		x								x			x	
HM00031	HERA000083	HM00031		x					x			x			x	
HM00032	HERA000084	Zinc phosphodiesterase		x							1	x			x	
HM00033	HERA000085	Serine/threonine-protein kinase (LMTK1)		x							8	x			x	
HM00034	HERA000086	WD repeat domain 13 (Wdr13)			1	4					5	x			x	
HM00035	HERA000087	Domeless			1	2						x			x	
HM00036	HERA000061	WAS protein family homologue 1			5	36					37	x			x	
HM00038	HERA000062	Lethal (2) k05819 CG3054										x	2		x	
HM00039	HERA000064	Mitogen-activated protein kinase (MAPKK)										x			x	
HM00040	HERA000064.1	DNA excision repair protein ERCC-6										x			x	
HM00041	HERA000065	Penguin										x			x	
HM00042	HERA000066	Thymidylate kinase										x			x	
HM00043	HERA000067	Caspase-activated DNase										x			x	
HM00044	HERA000068	Regulator of ribosome biosynthesis										x			x	
HM00045	HERA000069	CG12659										x			x	
HM00046	HERA000070	CG33505										x			x	
HM00047	HERA000071	Sr protein										x			x	
HM00048	HERA000073	HM00048										x			x	
HM00049	HERA000073.1	HM00049										x			x	
HM00050	HERA000074	Shuttle craft										x			x	
HM00051	HERA000075	HM00051										x			x	
HM00052	HERA000076	HM00052					x					x			x	

774

775 Yb^I, within the previously mapped *Yb* interval[12]. Sb^I, within the previously mapped *Sb*

776 interval[12]. *Sb* controls a white/yellow hindwing margin and is not investigated in this study.

777 The *N* locus has not been fine-mapped previously. A^{Yb}, number of above background SNPs

778 associated with the hindwing yellow bar in this study. A^{N}, number of above background
779 SNPs associated with the forewing yellow band in this study. E^{1}, detected as differentially
780 expressed between *Hm aglaope* and *amaryllis* from RNAseq data in this study
781 (Supplementary Information). E^{gw}, detected as differentially expressed between forewing
782 regions in the gene array in this study. E^{gr}, detected as differentially expressed between *Hm*
783 *plesseni* and *malleti* in in the gene array in this study. E^{tw}, numbers of probes showing
784 differential expression between forewing regions in the tilling array in this study. E^{tr},
785 numbers of probes showing differential expression between *Hm plesseni* and *malleti* in in the
786 tiling array in this study. Cr^{I}, within the previously mapped *HeCr* interval[11]. A^{pet}, number of
787 SNPs fixed for the alternative allele in *He demophoon*. A^{fav}, number of SNPs fixed for the
788 alternative allele in *He favorinus*. P^{I}, within the previously mapped P interval[13]. A^{bic}, number
789 of above background SNPs associated with the *Hn bicoloratus* phenotype in this study.
790

Extended Data Table 2. Locations of fixed/above background SNPs and differentially expressed (DE) tiling array probes

Positions of SNPs in the *He* and *Hn* association analyses	*cortex* coding exons	*cortex* UTR exons	*cortex* introns (nonTE)	*cortex* flanking intergenic (nonTE)	TEs	Other genes (exons or introns)	Other intergenic	Total
erato favorinus fixed	2	0	96	8	2	0	0	108
erato demophoon fixed	0	0	1	5	1	2	6	15
numata bicoloratus above background	1	3	47	16	0	2	0	69

Positions of DE tiling array probes			Known *cortex* coding exons	*cortex* UTR exons	*cortex* introns (nonTE)	miRNAs	TEs	Other gene exons	Other introns/ intergenic	Total
Day3	malleti vs plesseni	Forewing proximal	8	7	323	0	13	1	7	359
		Forewing distal	12	2	327	0	8	0	8	357
		Hindwing	5	14	378	0	9	1	6	413
	Proximal vs distal	malleti	0	1	68	0	0	0	12	81
		plesseni	2	4	222	0	10	0	4	242
Day1	malleti vs plesseni	Forewing proximal	1	0	22	0	3	0	7	33
		Forewing distal	2	3	116	1	9	5	112	248
		Hindwing	9	10	500	1	20	2	80	622
	Proximal vs distal	malleti	0	12	95	0	1	0	0	108
		plesseni	3	3	81	0	99	0	0	186

Extended Data Table 3. SNPs showing the strongest phenotypic associations in the *H. melpomene/timareta*/silvaniform comparison.

Species	Race	Sample Code	HW bar	SNP pos 457083† (p=6.07E-10)	SNP pos 439063* (p=1.72E-09)	SNP pos 602131‡ (p=2.42E-09)	SNP pos 457056† (p=2.42E-09)	FW band	SNP pos 584465§ (p=1.37E-07)	SNP pos 584418§ (p=1.41E-07)	SNP pos 584633§ (p=2.10E-07)	SNP pos 603344‡ (p=2.19E-07)
H. melpomene	*aglaope*	09-246	0	A/A	A/G	A/A	C/C	1	T/T	A/A	NA	T/T
H. melpomene	*aglaope*	09-267	0	A/A	G/G	A/A	C/C	1	T/T	A/A	C/C	T/T
H. melpomene	*aglaope*	09-268	0	A/A	G/G	A/A	C/C	1	T/T	A/A	C/C	T/T
H. melpomene	*aglaope*	09-357	0	A/A	G/G	G/A	C/C	1	T/T	NA	C/C	T/T
H. melpomene	*aglaope*	aglaope.1	0	A/A	G/G	NA	C/C	1	C/T	T/A	T/C	T/T
H. melpomene	*amandus*	2221	1	A/A	NA	G/G	C/C	0	C/C	T/T	T/T	A/A
H. melpomene	*amandus*	2228	1	A/A	NA	G/G	C/C	0	C/T	T/A	T/C	A/A
H. melpomene	*amaryllis*	09-332	1	T/T	A/A	G/G	T/T	0	C/C	T/T	T/T	A/A
H. melpomene	*amaryllis*	09-333	1	T/T	A/A	G/G	T/T	0	C/C	T/T	T/T	A/A
H. melpomene	*amaryllis*	09-075	1	T/T	A/A	G/G	T/T	0	C/C	T/T	T/T	A/A
H. melpomene	*amaryllis*	09-079	1	T/T	A/A	G/G	T/T	0	C/C	T/T	T/T	A/A
H. melpomene	*amaryllis*	amaryllis.1	1	T/T	A/A	G/G	T/T	0	C/C	T/T	T/T	A/A
H. melpomene	*bellula*	228	1	T/T	NA	G/G	T/T	0	C/C	T/T	T/T	NA
H. melpomene	*bellula*	231	1	T/T	NA	G/A	T/T	0	C/T	T/A	T/C	NA
H. melpomene	*cythera*	2856	1	T/T	A/A	G/G	T/T	0	C/C	T/T	T/T	A/A
H. melpomene	*cythera*	2857	1	NA	NA	NA	NA	0	NA	NA	NA	NA
H. melpomene	*malleti*	17162	0	A/A	G/G	A/A	C/C	1	T/T	A/A	C/C	T/T
H. melpomene	*melpomene*	18038	0	A/A	G/G	G/G	C/C	0	C/C	T/T	T/T	A/A
H. melpomene	*melpomene*	18097	0	NA	G/G	NA	C/C	0	C/C	T/T	T/T	NA
H. melpomene	*melpomene*	m0.06	0	A/A	G/G	G/G	C/C	0	C/C	T/T	T/T	A/A
H. melpomene	*melpomene*	gen_ref	0	A/A	G/G	NA	C/C	0	C/C	T/T	T/T	A/A
H. melpomene	*melpomene*	13435	0	A/A	G/G	A/A	C/C	0	C/C	T/T	T/T	A/A
H. melpomene	*melpomene*	9315	0	A/A	G/G	A/A	C/C	0	C/C	T/T	T/T	A/A
H. melpomene	*melpomene*	9316	0	A/A	G/G	A/A	C/C	0	C/C	T/T	T/T	A/A
H. melpomene	*melpomene*	9317	0	A/A	G/G	A/A	C/C	0	C/C	T/T	T/T	A/A
H. melpomene	*plesseni*	9156	0	A/A	G/G	A/A	C/C	0	C/C	T/T	T/T	NA
H. melpomene	*plesseni*	16293	0	A/A	G/G	A/A	C/C	0	C/C	T/T	T/T	NA
H. melpomene	*rosina*	rosina.1	1	T/T	A/A	G/G	T/T	0	C/C	T/T	T/T	A/A
H. melpomene	*rosina*	2071	1	T/T	A/A	G/G	T/T	0	C/C	T/T	T/T	A/A
H. melpomene	*rosina*	531	1	T/T	A/A	G/G	T/T	0	C/C	T/T	T/T	A/A
H. melpomene	*rosina*	533	1	T/T	NA	G/G	T/T	0	C/C	T/T	T/T	NA
H. melpomene	*rosina*	546	1	T/T	A/A	G/G	T/T	0	C/C	T/T	T/T	A/A
H. melpomene	*thelxiopeia*	13566	0	A/A	G/G	A/A	C/C	1	C/T	T/A	T/C	T/T
H. melpomene	*vulcanus*	14632	1	T/T	A/A	G/G	T/T	0	C/C	T/T	T/T	NA
H. melpomene	*vulcanus*	519	1	T/T	A/A	G/G	T/T	0	C/C	T/T	T/T	A/A
H. timareta	*florencia*	2403	0	A/A	G/G	A/A	C/C	1	T/T	A/A	C/C	T/T
H. timareta	*florencia*	2406	0	A/A	A/G	A/A	C/C	1	T/T	A/A	C/C	T/T
H. timareta	*florencia*	2407	0	A/A	A/G	A/A	C/C	1	T/T	A/A	C/C	T/T
H. timareta	*florencia*	2410	0	A/A	G/G	A/A	C/C	1	T/T	A/A	C/C	T/T
H. timareta	*timareta*	8533	0	A/A	G/G	A/A	C/C	1	C/T	T/A	T/C	T/T
H. timareta	*timareta*	9184	0	A/A	G/G	A/A	C/C	1	T/T	A/A	C/C	T/T
H. timareta	*timareta*	8520	0	A/A	G/G	A/A	C/C	1	T/T	A/A	C/C	T/T
H. timareta	*timareta*	8523	0	A/A	G/G	A/A	C/C	1	T/T	A/A	C/C	T/T
H. timareta	*thelxinoe*	09-312	1	T/T	A/A	G/G	T/T	0	C/C	T/T	T/T	A/A
H. timareta	*thelxinoe*	8624	1	T/T	A/A	G/G	T/T	0	C/C	T/T	T/T	A/A
H. timareta	*thelxinoe*	8628	1	T/T	A/A	G/G	T/T	0	C/C	T/T	T/T	A/A
H. timareta	*thelxinoe*	8631	1	T/T	A/A	G/G	T/T	0	C/C	T/T	T/T	A/A
H. elevatus		09-343	0	A/T	G/G	A/A	T/T	1	C/T	NA	C/C	T/T
H. pardalinus	*sergestus*	09-326	0	A/A	A/A	A/A	NA	0	C/C	T/T	T/T	NA

*downstream of *cortex*, †between exons 3 and 4 of *cortex*, ‡upstream of *cortex*, §between exons U4 and U3 of *cortex*. None of these SNPs are within known TEs. Colours show phenotypic associations: yellow = yellow hindwing bar; pink = no yellow hindwing bar;

green = yellow forewing band; blue = no yellow forewing band; grey = allele does not match expected pattern.

Extended Data Table 4. Transposable Elements (TEs) found within the *Yb* region.

Unique Occurrences									
BAC	mel	ros	ama	agl	No.	TE name	Superfamily		Type
1					1	BEL-1	BEL		LTR retrotransposon
					1	CR1-2	Jockey	LINE	Non-LTR retrotransposon
	1				1	Daphne-1	Jockey	LINE	Non-LTR retrotransposon
1					1	Daphne-6	Jockey	LINE	Non-LTR retrotransposon
1					1	DNA-like-8			DNA transposon
					1	Helitron-like-14	Helitron_A		DNA transposon
	1	2			4	Helitron-like-12	Helitron_A		DNA transposon
1	2				5	Helitron-like-12b	Helitron_A		DNA transposon
	1	1	1	1	7	Helitron-like-4a	Helitron_A		DNA transposon
						Helitron-like-4b	Helitron_A		DNA transposon
						Helitron-N2	Helitron_A		DNA transposon
					3	Helitron-like-7	Helitron_A		DNA transposon
5	3	3	1	2	16	Helitron-like-6a	Helitron_B		DNA transposon
						Helitron-like-6b	Helitron_B		DNA transposon
						Helitron-like-11	Helitron_B		DNA transposon
2	2	1		1	11	Helitron-like-15	Helitron_B		DNA transposon
6	5	3	1		18	Helitron-like-5	Helitron_B		DNA transposon
		1			2	Hmel_Unknown_50			
	1		1		2	Hmel_Unknown_174a/b			
	1				1	Hmel_Unknown_187b			
			1	1	2	Hmel_Unknown_230			
					1	Hmel_Unknown_234a			
					1	Hmel_Unknown_236a			
	1				1	Jockey-4	Jockey	LINE	Non-LTR retrotransposon
	1				1	LTR-3_gypsy	Gypsy		LTR retrotransposon
				1	1	Mariner-4	Mariner/Tc1		DNA transposon
1				3	29	Metulj-0	Metulj	SINE	Non-LTR retrotransposon
						Metulj-1	Metulj	SINE	Non-LTR retrotransposon
						Metulj-2	Metulj	SINE	Non-LTR retrotransposon
						Metulj-3	Metulj	SINE	Non-LTR retrotransposon
						Metulj-4	Metulj	SINE	Non-LTR retrotransposon
						Metulj-5	Metulj	SINE	Non-LTR retrotransposon
						Metulj-6	Metulj	SINE	Non-LTR retrotransposon
						Metulj-7	Metulj	SINE	Non-LTR retrotransposon
						nTc3-4	Mariner/Tc1		DNA transposon
						SINE-1	SINE	SINE	Non-LTR retrotransposon
1	1				2	nMar-3	Mariner/Tc1		DNA transposon
1					1	nMar-16	Mariner/Tc1		DNA transposon
			1		1	nMar-12/20	Mariner/Tc1		DNA transposon
				1	1	nPIF-3	PIF/Harbinger		DNA transposon
1					1	nTc3-2	Mariner/Tc1		DNA transposon
1					2	nTc3-3	Mariner/Tc1		DNA transposon
	1				2	R4-1	R2	LINE	Non-LTR retrotransposon
			1	1	6	Rep-1	REP	LINE	Non-LTR retrotransposon
2		1		1	4	RTE-3	RTE	LINE	Non-LTR retrotransposon
				1	2	RTE-11	RTE	LINE	Non-LTR retrotransposon
	1				3	Zenon-1	Jockey	LINE	Non-LTR retrotransposon
			1		1	Zenon-3	Jockey	LINE	Non-LTR retrotransposon